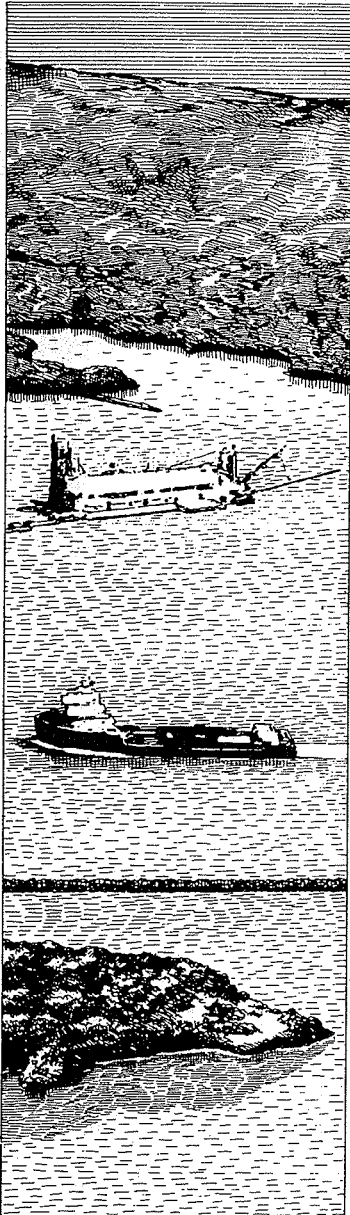


TA7  
W34  
no. DRP-92-6  
rept. 4

LIBRARY  
USE ONLY



## DREDGING RESEARCH PROGRAM

TECHNICAL REPORT DRP-92-6

# ADCIRC: AN ADVANCED THREE-DIMENSIONAL CIRCULATION MODEL FOR SHELVES, COASTS, AND ESTUARIES

## Report 4 HURRICANE STORM SURGE MODELING USING LARGE DOMAINS

by

C.A. Blain, J.J. Westerink

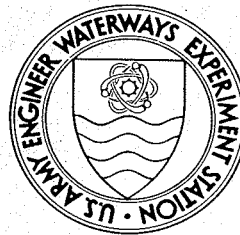
Department of Civil Engineering and Geological Sciences  
University of Notre Dame, Notre Dame, Indiana 46556

R.A. Luettich, Jr.

Institute of Marine Sciences  
University of North Carolina at Chapel Hill  
Morehead City, North Carolina 28557

Norman W. Scheffner

DEPARTMENT OF THE ARMY  
Waterways Experiment Station, Corps of Engineers  
3909 Halls Ferry Road, Vicksburg, Mississippi 39180-6199



August 1994

Report 4 of a Series

Approved For Public Release; Distribution Is Unlimited

Prepared for DEPARTMENT OF THE ARMY  
US Army Corps of Engineers  
Washington, DC 20314-1000

Under Work Unit 32466



The Dredging Research Program (DRP) is a seven-year program of the U.S. Army Corps of Engineers. DRP research is managed in these five technical areas:

- Area 1 - Analysis of Dredged Material Placed in Open Water
- Area 2 - Material Properties Related to Navigation and Dredging
- Area 3 - Dredge Plant Equipment and Systems Processes
- Area 4 - Vessel Positioning, Survey Controls, and Dredge Monitoring Systems
- Area 5 - Management of Dredging Projects

The contents of this report are not to be used for advertising, publication, or promotional purposes. Citation of trade names does not constitute an official endorsement or approval of the use of such commercial products.



PRINTED ON RECYCLED PAPER

USACEWES



3 5925 00260 2412



**US Army Corps  
of Engineers**  
Waterways Experiment  
Station

## Dredging Research Program Report Summary



### *ADCIRC: An Advanced Three-Dimensional Circulation Model for Shelves, Coasts, and Estuaries; Report 4: Hurricane Storm Surge Modeling Using Large Domains (TR DRP-92-6)*

**ISSUE:** A unified and systematic methodology must be provided to use in the investigation of the dispersive or nondispersive characteristics of a site proposed for the disposal of dredged material in open water as well as to analyze existing disposal sites.

**RESEARCH:** ADCIRC (Advanced Three-Dimensional Circulation Model) was developed as a part of the Dredging Research Program (DRP) as a means of generating a database of harmonic constituents for tidal elevation and current at discrete locations along the east, west, and Gulf of Mexico coasts and to utilize tropical and extratropical global boundary conditions to compute frequency-indexed storm surge hydrographs along the US coasts. The database is being developed to provide site-specific hydrodynamic boundary conditions for use in analyzing the long-term stability of existing or proposed dredged material disposal sites.

**SUMMARY:** This report describes an investigation of the use of large domains in

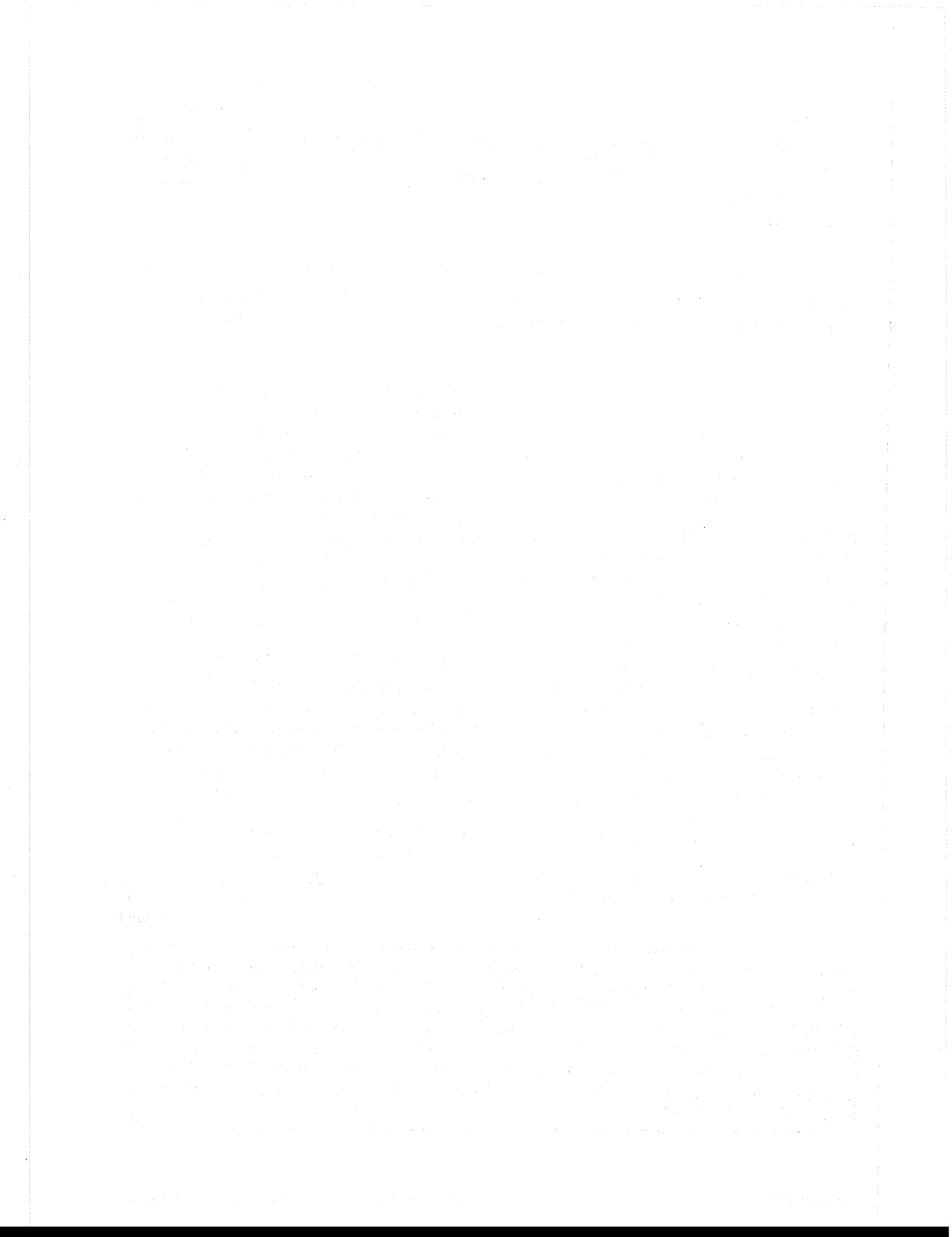
modeling hurricane storm surge. The hydrodynamic model used was the ADCIRC-2DDI code, which is based on a two-dimensional, depth integrated, finite element formulation. Hurricane wind stress and pressure forcing from Hurricane Kate (the 1985 historical storm modeled) were produced by the HURWIN code, a vertically averaged, planetary boundary layer wind model. The resulting storm surge elevations predicted at 8 stations along the Florida coast correlated well with measured storm surge elevations.

**AVAILABILITY OF REPORT:** The report is available through the Interlibrary Loan Service from the US Army Engineer Waterways Experiment Station (WES) Library, telephone number 601 634-2355. National Technical Information Service (NTIS) report numbers may be requested from WES Librarians.

To purchase a copy of the report, call NTIS at 703 487-4780.

RESEARCH LIBRARY  
US ARMY ENGINEER WATERWAYS  
EXPERIMENT STATION  
VICKSBURG, MISSISSIPPI

**About the Authors:** Dr. Norman W. Scheffner, Coastal Processes Branch of the Coastal Engineering Research Center's Research Division at the US Army Engineer Waterways Experiment Station, was the Principal Investigator for the DRP work unit. Dr. R. A. Luettich, Jr., Institute of Marine Sciences, University of North Carolina at Chapel Hill, and Dr. J. J. Westerink, Department of Civil Engineering, University of Notre Dame, assisted Dr. Scheffner in developing the modeling goals, concepts, and methodologies. Drs. Luettich and Westerink completed development and implementation of the model. For further information about the DRP, contact Mr. E. Clark McNair, Jr., Program Manager, at 601 634-2070.



31025577

TAN  
W34  
NO. DRP-92-6  
Rept. 4  
Technical Report DRP-92-6  
August 1994

**Dredging Research Program**

Technical Report DRP-92-6  
August 1994

# **ADCIRC: An Advanced Three-Dimensional Circulation Model for Shelves, Coasts, and Estuaries**

## **Report 4 Hurricane Storm Surge Modeling Using Large Domains**

by C.A. Blain, J.J. Westerink

Department of Civil Engineering and Geological Sciences  
University of Notre Dame, Notre Dame, IN 46556

R.A. Luettich, Jr.

Institute of Marine Sciences  
University of North Carolina at Chapel Hill  
Morehead City, NC 28557

Norman W. Scheffner

U.S. Army Corps of Engineers  
Waterways Experiment Station  
3909 Halls Ferry Road  
Vicksburg, MS 39180-6199

Report 4 of a series

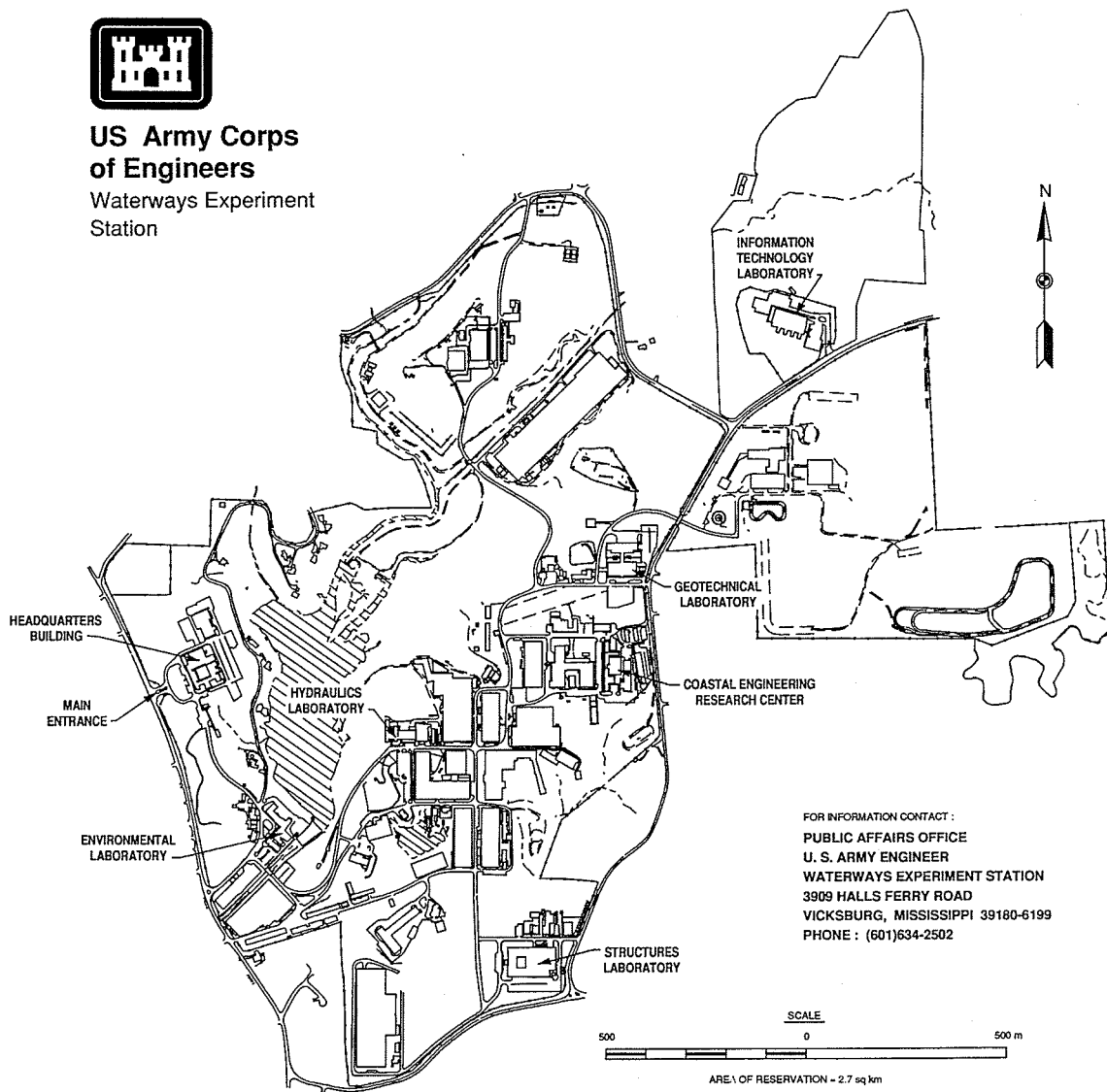
Approved for public release; distribution is unlimited

Prepared for U.S. Army Corps of Engineers  
Washington, DC 20314-1000

Under Work Unit 32466



**US Army Corps  
of Engineers**  
Waterways Experiment  
Station



FOR INFORMATION CONTACT :  
PUBLIC AFFAIRS OFFICE  
U. S. ARMY ENGINEER  
WATERWAYS EXPERIMENT STATION  
3909 HALLS FERRY ROAD  
VICKSBURG, MISSISSIPPI 39180-6199  
PHONE : (601)634-2502

### Waterways Experiment Station Cataloging-in-Publication Data

ADCIRC : An advanced three-dimensional circulation model for shelves, coasts, and estuaries. Report 4, Hurricane storm surge modeling using large domains / by C.A. Blain ... [et al.] ; prepared for U.S. Army Corps of Engineers.

63 p. : ill. ; 28 cm. -- (Technical report ; DRP-92-6 rept.4)

Includes bibliographic references.

"Report 4 of a series"--T.p.

1. Storm surges -- Mathematical models. 2. Ocean waves -- Mathematical models. 3. Finite element method. 4. Functions of complex variables. I. Blain, Cheryl Ann. II. United States. Army. Corps of Engineers. III. U.S. Army Engineer Waterways Experiment Station. IV. Dredging Research Program. V. Title: An advanced three-dimensional circulation model for shelves, coasts, and estuaries. VI. Title: Hurricane storm surge modeling using large domains. VII. Series: Technical report (U.S. Army Engineer Waterways Experiment Station) ; DRP-92-6 rept. 4. TA7 W34 no.DRP-92-6 rept.4

# Contents

---

Preface .....	vi
Conversion Factors, Non-SI to SI Units of Measurement .....	vii
Summary .....	viii
1—Introduction .....	1
2—Governing Equations and Numerical Discretization .....	4
3—Specification of Hurricane Wind Stress and Pressure Fields .....	9
4—Hurricane Kate Description .....	14
5—Comparison of Storm Surge Predictions Using Three Domains .....	16
Modeling Strategy .....	16
Computational Domain Descriptions .....	17
Storm Surge Simulations .....	25
6—Comparison Between Computed and Observed Storm Surge Elevations Using a Large Domain .....	39
7—Conclusions .....	49
References .....	51
SF 298	

## List of Tables

---

Table 1.	Properties of the Computational Domains .....	24
Table 2.	Tidal Potential Constants Used for Tidal and Storm Surge Simulations .....	40

## List of Figures

---

Figure 1.	Track of Hurricane Kate through the Western North Atlantic Ocean and into the Gulf of Mexico from November 15, 1985, 1800 GMT to November 23, 1985, 1800 GMT . . . . .	15
Figure 2.	Bathymetry contours in increments of 25, 50, 100, 200, 500, 1,000, 2,000, 3,000, 4,000, 5,000, 6,000, 7,000, and 8,000 m over the east coast domain . . . . .	18
Figure 3.	East coast domain discretization . . . . .	19
Figure 4.	Bathymetry contours in increments of 25, 50, 100, 200, 500, 1,000, 2,000, and 3,000 m over the Gulf of Mexico domain . .	21
Figure 5.	Gulf of Mexico domain discretization . . . . .	22
Figure 6.	Bathymetry contours in increments of 25, 50, 100, and 200 m over the Florida coast domain . . . . .	23
Figure 7.	Florida coast domain discretization . . . . .	23
Figure 8.	Names and locations of elevation stations in the Florida coast domain . . . . .	26
Figure 9.	Names and locations of elevation stations in the Gulf of Mexico domain . . . . .	27
Figure 10.	Names and locations of elevation stations in the east coast domain . . . . .	28
Figure 11.	Computed storm surge for Hurricane Kate at St. Marks, Florida, a) zero elevation open boundary condition, b) inverted barometer open boundary condition . . . . .	30
Figure 12.	Computed storm surge for Hurricane Kate at Turkey Point, Florida, a) zero elevation open boundary condition, b) inverted barometer open boundary condition . . . . .	31
Figure 13.	Computed storm surge for Hurricane Kate at Apalachicola, Florida, a) zero elevation open boundary condition, b) inverted barometer open boundary condition . . . . .	32
Figure 14.	Computed storm surge for Hurricane Kate at Panama City, Florida, a) zero elevation open boundary condition, b) inverted barometer open boundary condition . . . . .	33
Figure 15.	Computed storm surge for Hurricane Kate at Destin, Florida, a) zero elevation open boundary condition, b) inverted barometer open boundary condition . . . . .	34
Figure 16.	Computed storm surge for Hurricane Kate at Pensacola, Florida, a) zero elevation open boundary condition, b) inverted barometer open boundary condition . . . . .	35
Figure 17.	Comparison of computed storm surge for Hurricane Kate using an inverted barometer open boundary condition at Station 14 located on the Florida coast domain open boundary . . . . .	37



Figure 18.	Comparison of computed storm surge for Hurricane Kate using an inverted barometer open boundary condition at Station 20 located on the Florida coast domain open boundary . . . . .	37
Figure 19.	Comparison of computed storm surge for Hurricane Kate using an inverted barometer open boundary condition at Station 23 located on the Florida coast domain open boundary . . . . .	38
Figure 20.	Comparison of computed storm surge for Hurricane Kate over the east coast domain using both a zero elevation and an inverted barometer open boundary condition at St. Marks, Florida . . . . .	38
Figure 21.	Comparison of computed and measured tidal elevations over the east coast domain at Key West, Florida . . . . .	41
Figure 22.	Comparison of computed and measured tidal elevations over the east coast domain at Cedar Key, Florida . . . . .	42
Figure 23.	Comparison of computed and measured tidal elevations over the east coast domain at St. Marks Light, Florida . . . . .	42
Figure 24.	Comparison of computed and measured tidal elevations over the east coast domain at Alligator Bayou, Florida . . . . .	43
Figure 25.	Comparison of computed and measured tidal elevations over the east coast domain at Southwest Pass, Louisiana . . . . .	43
Figure 26.	Comparison of computed and measured tidal elevations over the east coast domain at Western Florida Outer Shelf . . . . .	44
Figure 27.	Comparison of computed and measured storm surge elevations for Hurricane Kate over the east coast domain at St. Marks, Florida . . . . .	44
Figure 28.	Comparison of computed and measured storm surge elevations for Hurricane Kate over the east coast domain at Turkey Point, Florida . . . . .	45
Figure 29.	Comparison of computed and measured storm surge elevations for Hurricane Kate over the east coast domain at Shell Point, Florida . . . . .	45
Figure 30.	Comparison of computed and measured storm surge elevations for Hurricane Kate over the east coast domain at Carrabelle, Florida . . . . .	46
Figure 31.	Comparison of computed and measured storm surge elevations for Hurricane Kate over the east coast domain at Apalachicola, Florida . . . . .	46
Figure 32.	Comparison of computed and measured storm surge elevations for Hurricane Kate over the east coast domain at Panama City, Florida . . . . .	47
Figure 33.	Comparison of computed and measured storm surge elevations for Hurricane Kate over the east coast domain at Destin, Florida . . . . .	47
Figure 34.	Comparison of computed and measured storm surge elevations for Hurricane Kate over the east coast domain at Pensacola, Florida . . . . .	48

# Preface

---

The work described in this report was authorized and funded under Work Unit No. 32466, "Numerical Simulation Techniques for Evaluating Long-Term Fate and Stability of Dredged Material Disposed in Open Water," of Technical Area 1 (TA1), Analysis of Dredged Material Placed in Open Water, of the Dredging Research Program (DRP), sponsored by Headquarters, U.S. Army Corps of Engineers (HQUSACE). Messrs. Robert Campbell and Glenn Drummond were DRP Chief and TA1 Technical Monitor from HQUSACE, respectively. Mr. E. Clark McNair, Jr., U.S. Army Engineer Waterways Experiment Station (WES), Coastal Engineering Research Center (CERC), was DRP Program Manager (PM), and Dr. Lyndell Z. Hales was Assistant PM. Dr. Nicholas C. Kraus, Research Division (RD), CERC, was the Technical Manager of the DRP TA1 and Dr. Norman W. Scheffner, Coastal Processes Branch (CPB), RD, CERC, was the Principal Investigator of Work Unit No. 32466. The numerical modeling goals, concepts, and methodologies were developed by Drs. Norman W. Scheffner, Joannes J. Westerink, and Richard A. Luetlich, Jr. Development and implementation of the model were completed by Drs. Westerink and Luetlich.

This study was performed and the report prepared over the period of 1 September 1992 through 31 March 1993. Dr. Scheffner was under the administrative supervision of Dr. James R. Houston, Director, CERC; Mr. Charles C. Calhoun, Jr., Assistant Director, CERC; Mr. H. Lee Butler, Chief, RD, CERC; and Mr. Bruce A. Ebersole, Chief, CPB, RD, CERC.

At the time of publication of this report, Director of WES was Dr. Robert W. Whalin. Commander was COL Leonard G. Hassell, EN.

Additional information on this report can be obtained from Mr. E. Clark McNair, Jr., DRP Program Manager, at (601)634-2070 or Dr. Norman W. Scheffner, Principal Investigator, at (601)634-3220.

*The contents of this report are not to be used for advertising, publication, or promotional purposes. Citation of trade names does not constitute an official endorsement or approval for the use of such commercial products.*

# Conversion Factors, Non-SI to SI Units of of Measurement

---

Non-SI units of measurement used in this report can be converted to SI units as follows:

<b>Multiply</b>	<b>By</b>	<b>To Obtain</b>
knots	0.5144444	meters per second
miles per hour	1.609347	kilometers per hour
millibars	1.0	kilopascals

# Summary

---

This report investigates the use of large domains in modeling hurricane storm surge. The hydrodynamic model used in this study is the ADCIRC-2DDI code which is based on a two-dimensional, depth-integrated, finite element formulation. Hurricane wind stress and pressure forcing from Hurricane Kate are produced by the HURWIN code, a vertically averaged planetary boundary layer wind model. Storm surge predictions are conducted over three computational domains each having a different size. The smallest domain is situated on the continental shelf, another domain covers the Gulf of Mexico, and the largest domain includes the Western North Atlantic Ocean, the Caribbean Sea, and the Gulf of Mexico. The largest domain is shown to be optimal for use with storm surge models. The influence of an inverted barometer condition applied at the open boundary is examined over each computational domain.

Both tidal and storm surge elevations are computed over the large scale domain. Tidal elevations compare well with measured tidal data at 77 stations. Storm surge predictions, which include both tidal and inverted barometer open boundary forcing, show excellent correlation with measured storm surge values when compared at eight stations along the Florida coast.

# 1 Introduction

---

The hurricane season of 1992 included such destructive and well publicized storms as Hurricane Andrew and Hurricane Iniki. Apart from the number of lives lost during these hurricanes, the costs due to material damage and disruption to local economies totalled into the billions of dollars. The devastation from these recent storms reinforces the fact that coastal flooding from hurricane storm surge remains a serious problem for seaside communities. In the interest of preventing loss of human life, the National Weather Service (NWS) issues warnings when hurricanes threaten U.S. coastal areas. NWS hurricane warnings contain information concerning the range of expected peak surge heights within the warning area (Jarvinen and Lawrence 1985). Computations made by a numerical storm surge model form the basis for NWS storm surge warnings (Jelenianski 1979). The U.S. Army Corps of Engineers also uses storm surge models to design coastal protection systems and to investigate the fate of dredged material disposed in the coastal environment. This report focuses on selection of an appropriate numerical storm surge model and its use in simulating hurricane storm surge.

Storm surge is a long-period wave caused by extreme wind and pressure forces. Water heights associated with storm surge are superimposed on water levels generated by tidal forcings. The period, wavelength, and amplitude characteristics of a storm surge depend on both geometric properties of the water body and characteristics of the meteorological forcing (Dendrou, Moore, and Myers 1985). A numerical model for storm surges must resolve the physical features which affect storm surge generation and propagation. Thus, an appropriate storm surge model incorporates complex coastal geometries, accounts for rapidly varying bathymetry in the continental slope and shelf regions, and permits reasonable boundary condition specification. During the course of development, storm surges and their associated forerunners encompass a large range of spatial scales. An acceptable numerical storm surge model must represent these scales of motion accurately so that energy in the system does not become artificially excited, and/or trapped within the system, and/or aliased in nonphysical ways.

A finite element (FE)-based numerical model with its inherent grid flexibility is selected as the ideal formulation for a storm surge model. Coastline detail is easily incorporated and nodal densities can range from three to four orders of magnitude. The wide variation in nodal density permits

significant refinement near coastal areas and in regions of rapid bathymetric changes and yet, the discrete problem remains well within computational limits. In this report, an FE-based storm surge model, ADCIRC-2DDI (Luettich, Westerink, and Scheffner 1992), which implements the wave-continuity equation (WCE) and momentum balance equations, is applied. The accuracy of these equations in solving various shallow-water problems is well-documented (Walters 1988; Werner and Lynch 1989; Walters and Werner 1989; Gray 1989; Foreman 1988; Lynch et al. 1989; Lynch and Werner 1991; Luettich, Westerink, and Scheffner 1992).

Aside from the numerical model, careful consideration must be given to the specification of wind stress and pressure at the water surface. Wind stress and pressure forcing are what drive the numerical storm surge model. As such, storm surge predictions are limited by the accuracy of the specified wind stress and pressure fields (Hubbert, Leslie, and Manton 1990; Dendrou, Moore, and Myers 1985; Flather 1984). A dynamic numerical model of the planetary boundary layer, which takes advantage of available meteorological data from historical storms, is chosen to compute the wind stress and pressure forcing (Cardone, Greenwood, and Greenwood 1992). This physically based wind model offers a more realistic representation of the meteorological forcing than more common empirical forms such as those described by Cardone, Greenwood, and Greenwood (1992) and those used by Johns et al. (1983a), Flather (1984), Jarvinen and Lawrence (1985), Hearn and Holloway (1990), and Westerink et al. (1992).

As noted by Jarvinen and Lawrence (1985), the initial design and location of the basin domain is a critical step in the construction of a storm surge model. Judicious location of a domain results in optimal storm surge calculations. Storm surge modeling efforts to date have primarily used domains which are limited to the continental shelf region and utilize finite difference methods with minimum grid flexibility (Hearn and Holloway 1990; Al-Rabeh, Eunay, and Cekirge 1990; Hubbert, Leslie, and Manton 1990; Lardner and Cekirge 1988; Dube, Sinha, and Roy 1986; Dendrou, Moore, and Myers 1985; Flather 1984; Johns et al. 1983a,b). Within the framework of finite differences, the need for grid refinement in near coastal regions is often accommodated by a nested grid approach. A small, finely discretized grid is contained within or coupled to a coarser regional grid (Hubbert, Leslie, and Manton 1990; Al-Rabeh, Eunay, and Cekirge 1990; Dendrou, Moore, and Myers 1985; Flather 1984). Near coastal continuous grid compression (Dube, Sinha, and Roy 1986; Johns et al. 1983a,b) is another technique also employed. While this technique more closely approaches the grid flexibility of the finite element method, the finite element method remains superior in its ability to accommodate discretization demands in an optimal fashion.

In this report, ADCIRC-2DDI, a WCE FE-based numerical storm surge model is used to investigate the role of the computational domain in accurate storm surge prediction. Storm surge is modeled over three computational domains, each spanning successively larger portions of the study area. A

comparison of storm surge predictions given by the model yields two major conclusions. First, a computational domain encompassing only the continental shelf grossly underpredicts hurricane storm surge and generally leads to erroneous values. Secondly, using a domain which extends into the deep ocean leads to the most accurate representation of the storm surge. On the continental shelf, both hurricane winds and the pressure deficit drive surface water up against the shoreline. Surface water elevations in the deep ocean, however, are mainly affected by the pressure deficit. Because the deep ocean pressure deficit is readily obtained and since the storm surge model is driven by surface water elevations specified at the open ocean boundary, use of surface elevations on a boundary located in the deep ocean yield better storm surge predictions. Tidal elevations at the open boundary in a large domain model can also be easily extracted from global tidal models. The interaction with waters adjacent to the region of interest is also important when modeling storm surge. A large domain includes these adjacent basins allowing all wavelengths associated with a storm surge to propagate throughout the domain and onto the continental shelf where development of storm surge is most critical. Thus, a large domain whose open boundary lies in the deep ocean is an optimal choice for storm surge prediction.

## 2 Governing Equations and Numerical Discretization

---

The computations described in this report were performed using ADCIRC-2DDI, the depth-integrated option of a system of two- and three-dimensional hydrodynamic codes named ADCIRC (Luettich, Westerink, and Scheffner 1992; Westerink et al. 1992b). ADCIRC-2DDI uses the depth-integrated equations of mass and momentum conservation, subject to the incompressibility, Boussinesq, and hydrostatic pressure approximations. Using the standard quadratic parameterization for bottom stress and neglecting baroclinic terms and lateral diffusion/dispersion effects leads to the following set of conservation statements in primitive nonconservative form expressed in a spherical coordinate system (Flather 1988; Kolar et al. 1992):

$$\frac{\partial \zeta}{\partial t} + \frac{1}{R \cos \phi} \left[ \frac{\partial UH}{\partial \lambda} + \frac{\partial (VH \cos \phi)}{\partial \phi} \right] = 0 \quad (1)$$

$$\begin{aligned} \frac{\partial U}{\partial t} + \frac{1}{R \cos \phi} U \frac{\partial U}{\partial \lambda} + \frac{1}{R} V \frac{\partial U}{\partial \phi} - \left( \frac{\tan \phi}{R} U + f \right) V = \\ - \frac{1}{R \cos \phi} \frac{\partial}{\partial \lambda} \left[ \frac{p_s}{\rho_0} + g(\zeta - \eta) \right] + \frac{\tau_{s\lambda}}{\rho_0 H} + \tau_{*U} \end{aligned} \quad (2)$$

$$\begin{aligned} \frac{\partial V}{\partial t} + \frac{1}{R \cos \phi} U \frac{\partial V}{\partial \lambda} + \frac{1}{R} V \frac{\partial V}{\partial \phi} + \left( \frac{\tan \phi}{R} U + f \right) U = \\ - \frac{1}{R} \frac{\partial}{\partial \phi} \left[ \frac{p_s}{\rho_0} + g(\zeta - \eta) \right] + \frac{\tau_{s\phi}}{\rho_0 H} - \tau_{*V} \end{aligned} \quad (3)$$

where

$t$  = time

$\lambda, \phi$  = degrees longitude (east of Greenwich positive) and degrees latitude (north of the equator positive)

$\zeta$  = free surface elevation relative to the geoid



$U, V$  = depth-averaged horizontal velocities  
 $R$  = radius of the Earth  
 $H = \zeta + h$  = total water column  
 $h$  = bathymetric depth relative to the geoid  
 $f = 2\Omega \sin\phi$  = Coriolis parameter  
 $\Omega$  = angular speed of the Earth  
 $p_s$  = atmospheric pressure at the free surface  
 $g$  = acceleration due to gravity  
 $\eta$  = effective Newtonian equilibrium tide potential  
 $\rho_0$  = reference density of water  
 $\tau_{sx}, \tau_{sy}$  = applied free surface stress  
 $\tau_* = C_f \frac{(U^2 + V^2)^{1/2}}{H}$   
 $C_f$  = bottom friction coefficient

A practical expression for the effective Newtonian equilibrium tide potential is given by Reid (1990) as:

$$\eta(\lambda, \phi, t) = \sum_{nj} \alpha_{jn} C_{jn} f_{jn}(t_0) L_j(\phi) \cos \left[ \frac{2\pi(t-t_0)}{T_{jn} + j\lambda + v_{jn}(t_0)} \right] \quad (4)$$

where

$C_{jn}$  = constant characterizing the amplitude of tidal constituent of species  $j$   
 $\alpha_{jn}$  = effective Earth elasticity factor for tidal constituent of species  $j$   
 $f_{jn}$  = time-dependent nodal factor  
 $v_{jn}$  = time-dependent astronomical argument  
 $j = 0, 1, 2$  = tidal species ( $j = 0$ , declinational;  $j = 1$ , diurnal;  $j = 2$ , semidiurnal)  
 $L_0 = 3\sin^2\phi - 1$   
 $L_1 = \sin(2\phi)$   
 $L_2 = \cos^2(\phi)$   
 $\lambda, \phi$  = degrees longitude and latitude, respectively  
 $t_0$  = reference time  
 $T_{jn}$  = period of constituent  $n$  of species  $j$

Values for  $C_{jn}$  are presented by Reid (1990). We note that the value for the effective Earth elasticity factor is typically taken as 0.69 for all tidal constituents (Schwidorski 1980; Hendershott 1981) although its value has been shown to be slightly constituent-dependent (Wahr 1981; Woodworth 1990).

To facilitate an FE solution to Equations 1-3, these equations are mapped from spherical form into a rectilinear coordinate system using a Carte Parallelogrammatique (CP) projection (Pearson 1990):

$$x' = R(\lambda - \lambda_0) \cos \phi_0 \quad (5)$$

$$y' = R\phi \quad (6)$$

where

$\lambda_0, \phi_0$  = center point of the projection

Applying the CP projection to Equations 1-3 gives the shallow water equations in primitive nonconservative form expressed in the CP coordinate system:

$$\frac{\partial \zeta}{\partial t} + \frac{\cos \phi_0}{\cos \phi} \frac{\partial(UH)}{\partial x'} + \frac{1}{\cos \phi} \frac{\partial(VH \cos \phi)}{\partial y'} = 0 \quad (7)$$

$$\begin{aligned} \frac{\partial U}{\partial t} + \frac{\cos \phi_0}{\cos \phi} U \frac{\partial U}{\partial x'} + V \frac{\partial U}{\partial y'} - \left( \frac{\tan \phi}{R} U + f \right) V = \\ - \frac{\cos \phi_0}{\cos \phi} \frac{\partial}{\partial x'} \left[ \frac{p_s}{\rho_0} + g(\zeta - \eta) \right] + \frac{\tau_{s\lambda}}{\rho_0 H} + -\tau_* U \end{aligned} \quad (8)$$

$$\begin{aligned} \frac{\partial V}{\partial t} + \frac{\cos \phi_0}{\cos \phi} U \frac{\partial V}{\partial x'} + V \frac{\partial V}{\partial y'} + \left( \frac{\tan \phi}{R} U + f \right) U = \\ - \frac{\partial}{\partial y'} \left[ \frac{p_s}{\rho_0} + g(\zeta - \eta) \right] + \frac{\tau_{s\phi}}{\rho_0 H} - \tau_* V \end{aligned} \quad (9)$$

Utilizing the FE method to resolve the spatial dependence in the shallow-water equations in their primitive form gives inaccurate solutions with severe artificial near  $2 \times \Delta x$  modes (Gray 1982). However, reformulating the primitive equations into a Generalized Wave Continuity Equation (GWCE) form gives highly accurate, noise-free, FE-based solutions to the shallow-water equations (Lynch and Gray 1979; Kinnmark 1984). The GWCE is derived by combining a time-differentiated form of the primitive continuity equation and a spatially differentiated form of the primitive momentum equations. The result is recast into conservative form, reformulating the convective terms into nonconservative form, and adding the primitive form of the continuity equation multiplied by a constant in time and space,  $\tau_0$  (Lynch and Gray 1979; Kinnmark 1984; Luetlich, Westerink, and Scheffner 1992). The GWCE in the CP coordinate system is:

$$\begin{aligned}
& \frac{\partial^2 \zeta}{\partial t^2} + \tau_0 \frac{\partial \zeta}{\partial t} + \frac{\cos \phi_0}{\cos \phi} \frac{\partial}{\partial x'} \frac{\partial \zeta}{\partial t} \left\{ U - \frac{\cos \phi_0}{\cos \phi} UH \frac{\partial U}{\partial x'} \right. \\
& - VH \frac{\partial U}{\partial y'} + \left( \frac{\tan \phi}{R} U + f \right) VH - H \frac{\cos \phi_0}{\cos \phi} \frac{\partial}{\partial x'} \left[ \frac{p_s}{\rho_0} + g(\zeta - \eta) \right] \\
& \left. - (\tau_* - \tau_0)UH + \frac{\tau_{s\lambda}}{\rho_0} \right\} \\
& + \frac{\partial}{\partial y'} \left\{ V \frac{\partial \zeta}{\partial t} - \frac{\cos \phi_0}{\cos \phi} UH \frac{\partial v}{\partial x'} - VH \frac{\partial v}{\partial y'} - \left( \frac{\tan \phi}{R} U + f \right) UH \right. \\
& \left. - H \frac{\partial}{\partial y'} \left[ \frac{p_s}{\rho_0} + g(\zeta - \eta) \right] - (\tau_* - \tau_0) VH + \frac{\tau_{s\phi}}{\rho_0} \right\} \\
& - \frac{\partial}{\partial t} \left( \frac{\tan \phi}{R} VH \right) + -\tau_0 \left( \frac{\tan \phi}{R} VH \right) = 0 \tag{10}
\end{aligned}$$

The GWCE (Equation 10) is solved in conjunction with the primitive momentum equations in nonconservative form, Equations 8 and 9.

The high accuracy of GWCE-based FE solutions is a result of their excellent numerical amplitude and phase propagation characteristics. In fact, Fourier analysis indicates that in constant-depth water, by using linear interpolation, a linear tidal wave resolved with 25 nodes per wavelength is more than adequately resolved over the range of Courant numbers,  $C = \sqrt{gh}\Delta t/\Delta x \leq 1.0$  (Luettich, Westerink and Scheffner 1992). Furthermore, the monotonic dispersion behavior of GWCE-based FE solutions avoids generating artificial near  $2 \times \Delta x$  modes, which plague primitive-based FE solutions (Platzman 1981; Foreman 1983). The monotonic dispersion behavior of GWCE-based FE solutions is very similar to that associated with staggered finite difference solutions to the primitive shallow-water equations (Westerink and Gray 1991). GWCE-based FE solutions to the shallow-water equations allow for extremely flexible spatial discretizations, which result in a highly effective minimization of the discrete size of any problem (Le Provost and Vincent 1986; Foreman 1988; Vincent and Le Provost 1988; Westerink et al. 1992).

The details of ADCIRC, an application of the GWCE-based solution to the shallow-water equations, are described by Luetich, Westerink, and Scheffner (1992). As most GWCE-based FE codes, ADCIRC applies three-noded linear triangles for surface elevation, velocity, and depth. Furthermore, decoupling of the time and space discrete form of the GWCE and momentum equations, time-independent and/or tri-diagonal system matrices, and full vectorization of all major loops results in a highly efficient code. It is noted that wetting and/or drying of elements is not currently accommodated by ADCIRC.

### 3 Specification of Hurricane Wind Stress and Pressure Fields

---

In most studies, very simple descriptions of the hurricane wind field are used to drive sophisticated hydrodynamic numerical models. This disparity severely limits validation of these coastal ocean models and puts into question the usefulness of results obtained from such models. In order to reduce the uncertainties caused by a poorly specified wind and pressure field, this study incorporates a wind model based on the basic physical and dynamic characteristics of a tropical cyclone.

Wind stress and pressure computations throughout this report were carried out by a modified form of the HURWIN model. The HURWIN model, part of the Coastal Modeling System at the U.S. Army Corps of Engineers Waterways Experiment Station, is based on the vortex model of Chow (1971) modified by Cardone, Greenwood, and Greenwood (1992). A time history of the surface wind field, based on available data from historical hurricanes, is the end product of the HURWIN model. The theoretical basis of the HURWIN model is the equation of horizontal motion, vertically averaged through the depth of the planetary boundary layer (PBL), expressed in coordinates fixed to the Earth:

$$\frac{dV}{dt} + f\hat{k} \times V = -\left(\frac{1}{\rho} \nabla P\right) + \nabla \cdot K_H \nabla V + \left(-\frac{C_D}{h}\right)|V|V \quad (11)$$

where

$$\frac{d}{dt} = \frac{\partial}{\partial t} + V \cdot \nabla$$

$$\frac{\partial}{\partial t} = \text{local time change relative to fixed coordinates}$$

$$\nabla = \text{two-dimensional del operator}$$

$$V = \text{vertically averaged horizontal wind velocity}$$

$$f = \text{Coriolis parameter}$$

$\hat{k}$  = unit vector in the vertical direction  
 $\rho_{air}$  = mean air density  
 $P$  = depth-averaged pressure in the PBL  
 $K_H$  = horizontal eddy viscosity coefficient  
 $C_D$  = surface drag coefficient  
 $h$  = depth of the planetary boundary layer

The vertical advection of momentum is assumed to be small compared to the horizontal advection and is thus neglected. Additionally, the shear stress at the top of the PBL is taken to be zero.

Total pressure is prescribed to be a sum of the pressure associated with the tropical cyclone  $P_c$  which is translating with the storm at a speed  $V_c$  and a large-scale background pressure  $\bar{P}$ :

$$P = P_c + \bar{P} \quad (12)$$

The background or far-field pressure can be specified in terms of a corresponding geostrophic flow as:

$$f\hat{k} \times V_g = -\left(\frac{1}{\rho} \nabla \bar{P}\right) \quad (13)$$

where  $V_g$  is the constant geostrophic velocity. Substituting in the pressure relationships in Equations 12 and 13 into Equation 11, the integrated wind field within the PBL becomes:

$$\frac{dV}{dt} + f\hat{k} \times (V - V_g) = -\left(\frac{1}{\rho} \nabla P_c\right) + \nabla \cdot K_H \nabla V + \left(-\frac{C_D}{h}\right) |V|V \quad (14)$$

The governing equations used in the HURWIN model are formed by transforming Equation 14 to a moving Cartesian coordinate system whose origin is located at the low pressure center of the storm.

A boundary condition appropriate for Equation 14 remains to be defined. Noting that the acceleration and horizontal diffusion of momentum at the edges of the computational domain are neglected, a balance is implied between the Coriolis force, the pressure gradient force, and the surface frictional force at these boundaries.

Specification of the pressure field for a tropical cyclone  $P_c$  is accomplished using the well-known exponential pressure law:

$$P_c = P_{eye} + \Delta p e^{-(R/r)} \quad (15)$$

where

$P_{eye}$  = pressure at the center or eye of the storm

$\Delta p$  = pressure anomaly,  $\bar{P} - P_{eye}$

$R$  = scale radius, often assumed equivalent to the radius to the maximum wind

$r$  = radial distance from the eye of the storm

This simple but widely used form applies to a radially symmetric pressure field. An option is available in which the pressure anomaly  $\Delta p$  and the radius to maximum wind  $R$  can be specified by storm quadrant. With this option, an asymmetrical pressure field results after smoothing between the pressure variations specified for each quadrant. The theoretical basis of the PBL hurricane wind model, HURWIN, is only briefly outlined here. A more extensive description is given by Cardone, Greenwood, and Greenwood (1992).

The computational scheme employed by the HURWIN model involves a nested grid system consisting of five rectangular grids each with a uniform mesh spacing. This mesh spacing doubles for successively larger grids. For instance, if the innermost grid has a spacing of 5 km, the remaining grids have mesh sizes of 10 km, 20 km, 40 km, and 80 km. Thus, the maximum areal extent of the nested grid system for this example is 1,600 km<sup>2</sup>. The grid system is centered at the eye of the storm and moves with the storm throughout the domain as dictated by the form of the governing equations. The numerical discretization of the governing equations is based on a finite difference formulation, the details of which are given by Chow (1971).

The HURWIN model is based on the concept that a tropical storm generally changes structure relatively slowly. For example, the structure of a hurricane travelling over open water can usually be well-represented by parameters specified at intervals of 6 to 24 hr. These representative states are the "snapshots" of the wind field. Parameters which must be specified for a given snapshot include: pressure at the eye of the storm, far-field pressure, radius to maximum wind, storm track direction, speed of the storm, surface geostrophic wind velocity, direction of the surface geostrophic wind, and mesh spacing of the innermost grid. Although the structure typically changes slowly, storm position can change relatively quickly. Differences in the time scale between storm structure and position changes are accommodated by specifying the storm center at every hour. The hourly information needed includes the latitude and longitude of the storm center and the relative weighting between snapshots which bracket a given hour. The snapshot and hourly data required for operation of the HURWIN model are obtained from commonly available meteorological data for historical hurricanes. The full time history of the surface wind field is then obtained by linear interpolation in time using this series of characteristic wind-field snapshots. The snapshots are calculated at discrete times during the course of the storm using steady state assumptions.

Despite the more realistic theoretical basis of the HURWIN model, several limitations arise in the model's ability to represent the hurricane wind field. The most prominent shortcoming relates to the lack of dissipation in the wind field of a hurricane making landfall. As a hurricane approaches land, it generally slows and winds dissipate. Consequently, winds on the right side of the hurricane are somewhat reduced from full strength as they encounter the land. As the winds rotate over the land, their speed is further reduced by frictional forces due to the roughness of the land. Thus, winds on the left side of the hurricane coming off the land are significantly less in magnitude than they were upon initially encountering land. The PBL wind model does not represent these processes associated with a hurricane making landfall. This limitation of the PBL hurricane wind model leads to drying of coastal elements on the left side of the hurricane and overprediction of peak surge on the right side of the hurricane.

Note that the HURWIN model does accommodate terrains of varying roughness. Upon incorporation of surface roughness variations, the winds over land are reduced by a constant factor. But, as the winds come off the land and into the open water, the wind speed will uniformly increase in accordance with the reduced friction of the open ocean. This is not a physically realistic representation of the wind field in a hurricane as it approaches landfall. Left- and right-side differences in the wind structure are not addressed by this feature in the PBL hurricane wind model. For simulations presented in this report, all surface roughness parameters pertain to the open ocean.

One final option available in the HURWIN model, which is not utilized, is the specification of an asymmetrical storm pressure field. Hurricanes in this report are represented by radially symmetric pressure profiles. Lack of detailed data precludes consideration of an asymmetrical hurricane pressure representation.

As mentioned previously, the HURWIN model has been slightly modified so as to directly interface with the ADCIRC-2DDI hydrodynamic model. One addition is that wind speeds computed over the nested grid system are converted to surface wind stresses using the relationship proposed by Garratt (1977):

$$\frac{\tau_x}{\rho_0} = C_D \frac{\rho_{air}}{\rho_0} |W| W_x \quad (16)$$

and

$$\frac{\tau_y}{\rho_0} = C_D \frac{\rho_{air}}{\rho_0} |W| W_y \quad (17)$$



where

$\tau_x, \tau_y$  = wind stress in the  $x$  and  $y$  directions, respectively

$\rho_{air}/\rho_w$  = ratio of air density to average density of seawater, 0.001293

$C_D$  = frictional drag coefficient, computed  $(0.75 + 0.067W)0.001$

$|W|$  = magnitude of wind velocity

$W_x, W_y$  = components of the wind velocity vector in the  $x$  and  $y$  directions, respectively

In the HURWIN model, pressure is not explicitly computed, but rather the pressure gradient is determined. The ADCIRC model, however, requires as input a pressure field expressed as an equivalent height of water  $P/(\rho_w g)$ . Thus, the HURWIN model has been adjusted to produce a field of  $P/(\rho_w g)$  over the nested grids. Both wind stresses and  $P/(\rho_w g)$  values are linearly interpolated directly from the PBL nested grids onto the finite element computational grid used by the ADCIRC model. All modifications to the HURWIN model result in an output of hourly wind stress and  $P/(\rho_w g)$  values at all nodal points in the ADCIRC computational grid.

## 4 Hurricane Kate Description

---

For the storm surge domain studies conducted in this report, Hurricane Kate is the historical storm modeled. The track of Hurricane Kate through the Western Atlantic Ocean and the Gulf of Mexico is shown in Figure 1 for 1-hr increments. Beginning in the deep Western Atlantic Ocean, Hurricane Kate was recognized as a tropical storm at 1800 GMT on November 15, 1985. The storm was upgraded 24 hr later to a hurricane as winds reached over 80 mph.<sup>1</sup> A minimum pressure of 953 mb and a maximum sustained wind speed of about 121 mph were recorded 26.5 hr prior to landfall as Kate moved northeastward through the Gulf of Mexico. Landfall of Hurricane Kate occurred at 2230 GMT on November 21, 1985, near Panama City, Florida. The tracking of Hurricane Kate continued through 1800 GMT, November 23, 1985, until the storm had significantly dissipated and was classified as an extratropical storm. Extensive meteorological analysis of Hurricane Kate as well as hydrographs depicting the storm surge analysis at ten stations along the Florida coast in the vicinity of Panama City can be found in the report by Garcia and Hegge (1987).

Wind stress and pressure forcing for the ADCIRC-2D simulations are computed using the HURWIN model. Beginning at 1800 GMT, November 15, 1985, and ending 8 days later at 1800 GMT, November 23, 1985, 193 total hours of Hurricane Kate are simulated. During this period, the forward speed of Hurricane Kate ranged from 3 to 26 knots. The far field pressure of 1,013 mb was taken to be constant throughout the simulation. The radius to maximum wind varied from a maximum of 41 km during hurricane development to a low of 9 km during peak intensity of the storm. Finally, the innermost nested grid spacing is set at 5 km, which leads to 1,600 km<sup>2</sup> of areal coverage by the nested grids about the eye of the hurricane.

---

<sup>1</sup> A table of factors for converting non-SI units of measurement to SI units is presented on page vii.

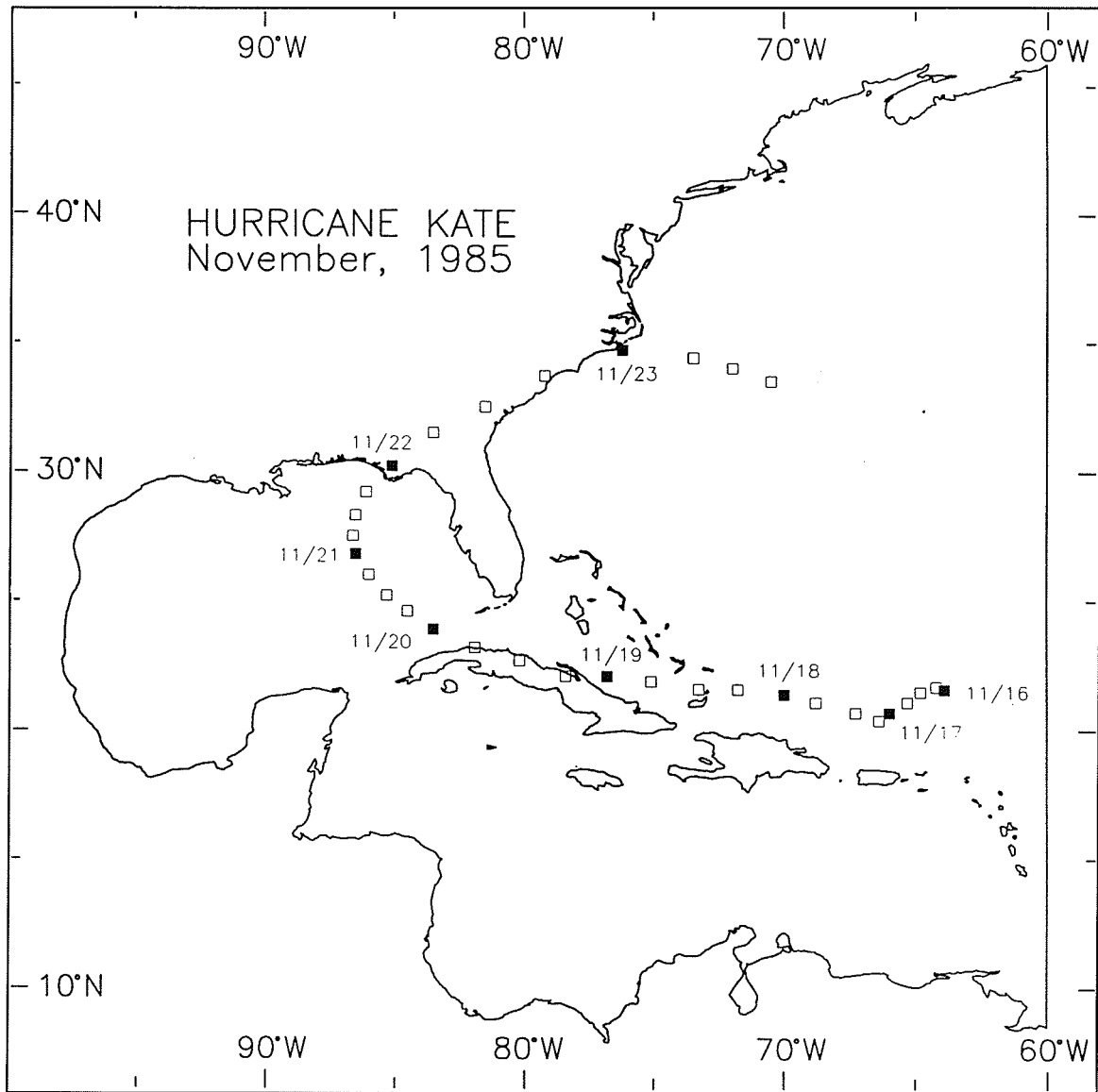


Figure 1. Track of Hurricane Kate through the Western North Atlantic Ocean and into the Gulf of Mexico from November 15, 1985, 1800 GMT to November 23, 1985, 1800 GMT

## 5 Comparison of Storm Surge Predictions Using Three Domains

---

A numerical storm surge model is comprised of several major components: the governing equations, a numerical discretization, wind and pressure forcing, and a computational domain. All of these components can significantly affect the ability of a model to make accurate predictions. Westerink et al. (1992) previously demonstrated the capabilities of the ADCIRC-2D model with regards to the governing equations and numerical discretization. In this study, the role of the computational domain in storm surge prediction is investigated through consideration of three different domains. Each domain telescopes outward from the landfall location of Hurricane Kate and covers successively larger areas.

### Modeling Strategy

As mentioned previously, most storm surge modeling efforts to date have used domains which extend only over the continental shelf region. Physically, though, appreciable development of the storm surge occurs as it moves up the continental slope and onto the shelf. This suggests that shelf models are not optimal for storm surge prediction. In the work of Westerink et al. (1992), a domain comprised of the entire Gulf of Mexico is used. Certainly this domain is an improvement over one restricted to the continental shelf, but the Gulf of Mexico is plagued by resonant frequencies well documented by Bungapong, Reid, and Whitaker (1985). These resonant modes are easily excited by the shape and size of the domain, artifacts in the domain discretization, forcing functions, and/or, the boundary conditions and can interfere with an accurate representation of a hurricane storm surge. A very large domain which extends into the deep ocean is ideal. A hurricane can progress through the domain generating and propagating storm surge in a more natural and realistic fashion. An extensive domain more fully incorporates the factors affecting storm surge generation (i.e., the bathymetry, wind and pressure forcing, and the influence of adjacent basins). In the deep ocean, changes in surface water elevation relate mainly to pressure deficits and not wind forcing, so for the large domain

model, an inverted barometer condition applied at the open boundary is reasonable. An inverted barometer  $P/(\rho_w g)$  is simply the height to which the seawater will rise due to pressure forcing. In shallow waters, storm surge is generated by a complex interaction between bathymetry, coastline geometry, and wind forcing. Thus, an inverted barometer condition applied over shallow waters does not accurately represent surface water elevations due to hurricane forcing. Any errors due to the erroneous specification of boundary forcing due to a storm are minimized for the large domain model since the open ocean boundary is located quite far from the coastal region of interest. Finally, for a large domain model, tidal elevation data can easily be obtained from global ocean models.

## Computational Domain Descriptions

The largest domain, the east coast domain shown in Figure 2, encompasses the Western North Atlantic Ocean, the Caribbean Sea, and the Gulf of Mexico. The east coast domain includes an open ocean boundary which extends from Glace Bay, Nova Scotia, to the vicinity of Corocora Island in eastern Venezuela along the 60°W meridian. All other boundaries are defined by the eastern coastlines of North, Central, and South America. Topography within the domain, depicted in Figure 2, includes the continental shelf, whose depths range from an imposed minimum of 3 m to 7 m (Westerink, Luettich, and Scheffner 1993) to 130 m, the continental slope which has a typical depth range of 130 m to 3,000 m, and the continental rise and deep ocean where bathymetries range from 3,000 m upwards to almost 8,000 m. Bathymetry in the Gulf of Mexico is specified to be in accordance with the detailed database used by Westerink et al. (1992).

The east coast domain discretization, shown in Figure 3, is based on Grid V3 created by Westerink, Luettich, and Scheffner (1993) for the Western North Atlantic Tidal model. Changes to Grid V3 include refinement by a factor of two in the interior regions of the Gulf of Mexico and the deep ocean. Also, the coastline and coastal waters surrounding Panama City, Florida, the region where Hurricane Kate made landfall, have been substantially refined. The approximate nodal spacing for the east coast domain discretization varies according to region. As an example, the grid size in coastal areas is approximately 0.006°, while in the deep ocean, spacing is about 1.15°. The east coast domain discretization is constructed with 22,711 nodes and 41,709 elements, reasonable numbers considering the level of refinement and the areal extent of the domain. Optimal gridding and the flexibility of the FE method make such a large computational problem manageable. Resolution of the domain can be expressed using an  $M_2$  wavelength-to-grid size ratio  $\lambda_{M_2}/\Delta_x$ , which is a measure of the number of nodal points used to resolve a wavelength of the  $M_2$  tide. A minimum criterion for resolution of the  $M_2$  tide is  $\lambda_{M_2}/\Delta_x$  equal to 12.5. The  $\lambda_{M_2}/\Delta_x$  ratio for the east coast domain ranges from approximately 15 to 1,336.



Figure 2. Bathymetry contours in increments of 25, 50, 100, 200, 500, 1,000, 2,000, 3,000, 4,000, 5,000, 6,000, 7,000, and 8,000 m over the east coast domain

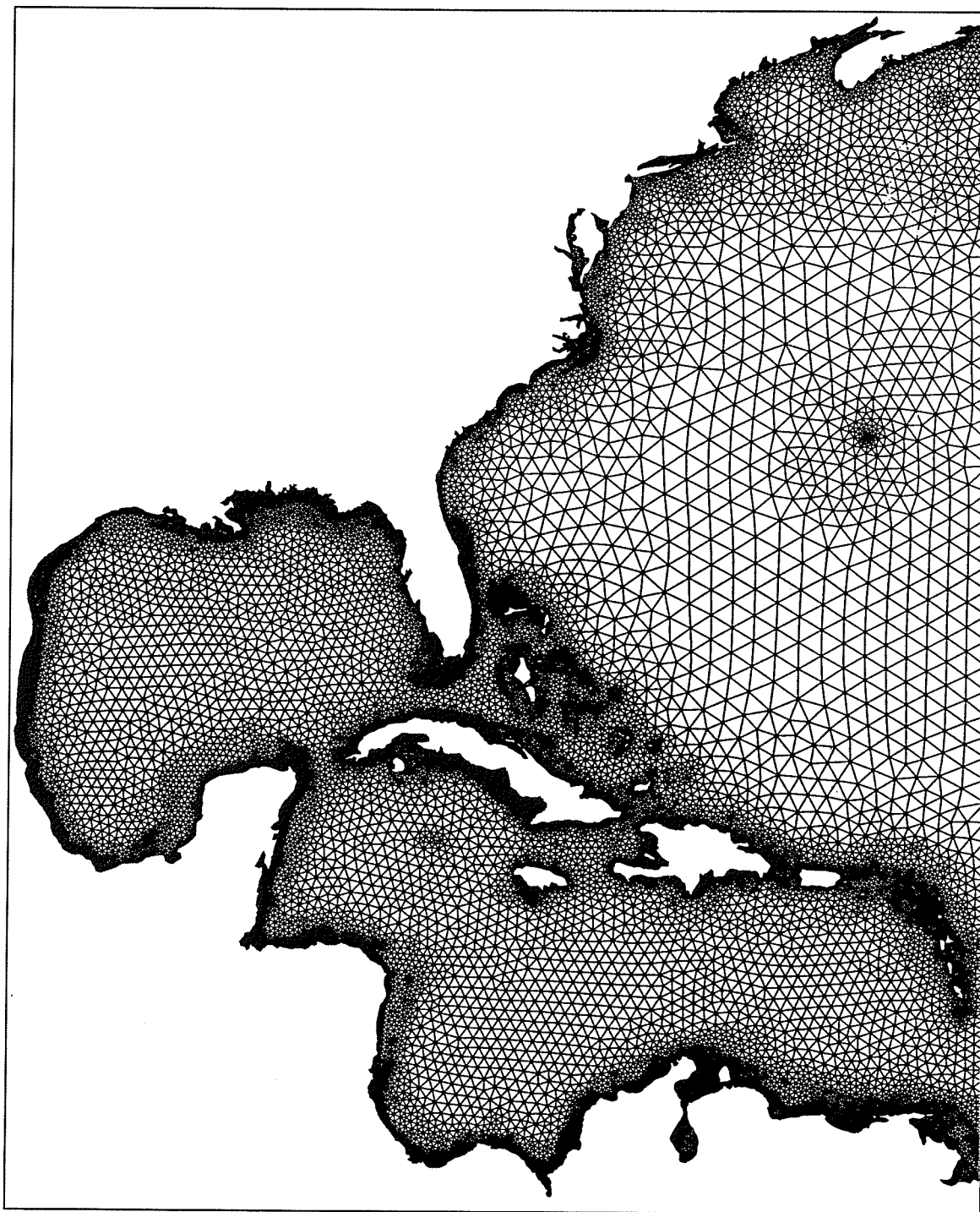


Figure 3. East coast domain discretization

The second computational domain, the Gulf of Mexico, is shown in Figure 4. This domain is extracted directly from the east coast domain and includes the entire Gulf of Mexico. Within the Gulf of Mexico domain, two well-defined open ocean boundaries exist. One is constructed across the Strait of Florida extending approximately from Cape Sable, FL, to Havana, Cuba. The second open ocean boundary stretches across the Yucatan Channel in the vicinity of Cancun, Mexico, and Cabo San Antonio, Cuba. The bathymetry, displayed in Figure 4, for the Gulf of Mexico domain is exactly the same as that specified for the Gulf of Mexico region within the east coast domain. Again for simulation purposes, a minimum depth of 3 m is imposed and the maximum depth in the Gulf of Mexico domain is just under 3,800 m. The Gulf of Mexico domain discretization entails 6,325 nodes and 11,441 elements and is presented in Figure 5. Approximate nodal spacings of the discretization range from a maximum of  $0.64^\circ$  to a minimum of  $0.006^\circ$  and the resolution, given by values of  $\lambda_{M_2}/\Delta_x$ , varies between 15 and 721 grid points per wavelength of the  $M_2$  tide.

The final domain under study, the Florida coast, pictured in Figure 6, is the smallest and is confined to the continental shelf. The Florida coast domain is cut directly out of the Gulf of Mexico domain and spans the coastline from St. Marks, FL, to the Mississippi Sound, reaching outwards to the edge of the continental shelf. The open-ocean boundaries can be delineated by three connected segments. Two of the segments project into the open water from the coastline, a western boundary segment beginning near Biloxi, MS, and an eastern boundary segment intersecting the coastline halfway between St. Marks and Cedar Key, FL. Both of these straight line segments connect with an arcing open ocean boundary, which loosely follows the edge of the continental shelf, approximately 100-200 m. Bathymetry values given in Figure 6 range from the minimum of 3 m to nearly 240 m. The Florida coast domain has a discretization of 1,933 nodes and 3,145 elements (see Figure 7) and a  $\lambda_{M_2}/\Delta_x$  range of 27 to 597 grid points per wavelength.

Properties of each of the three computational domains under study are summarized in Table 1. The region of interest, when considering the storm surge from Hurricane Kate, is the Florida coast surrounding the point of landfall near Panama City, FL. It is noted that the NWS uses a standard semicircular domain, the Pensacola Bay basin (Jarvinen and Lawrence 1985), which corresponds roughly to the Florida coast domain used in this study.



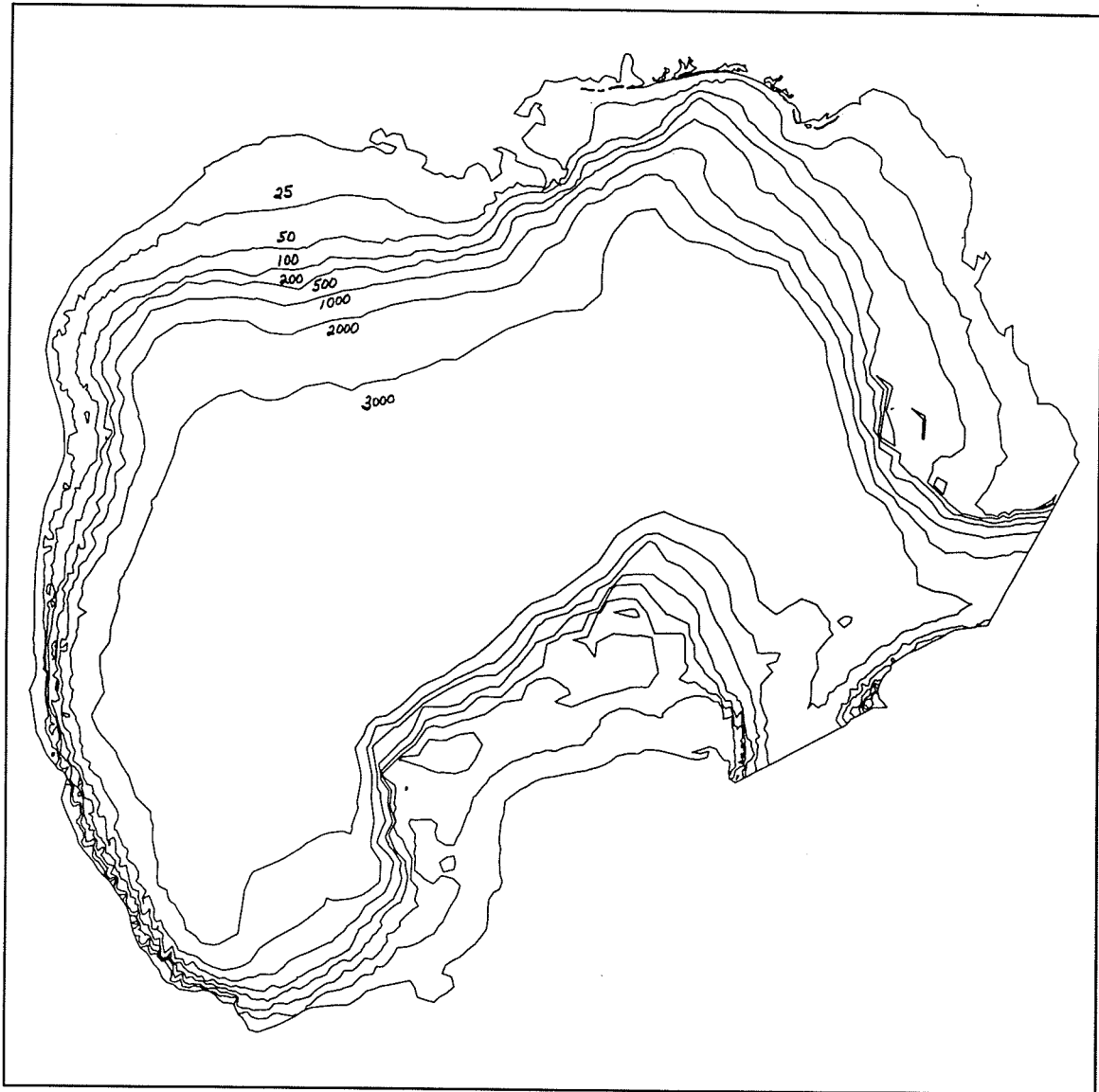


Figure 4. Bathymetry contours in increments of 25, 50, 100, 200, 500, 1,000, 2,000, and 3,000 m over the Gulf of Mexico domain

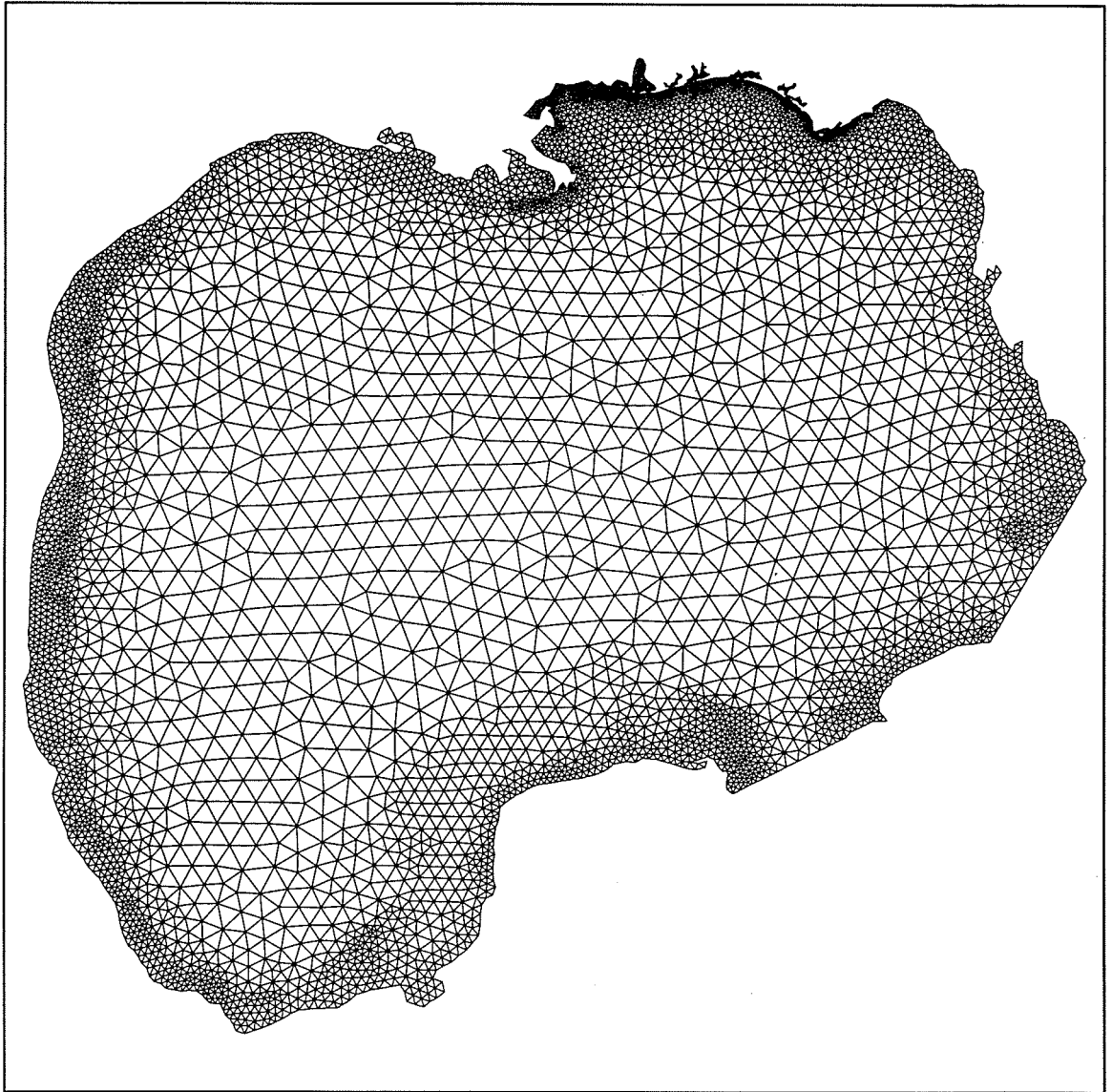


Figure 5. Gulf of Mexico domain discretization

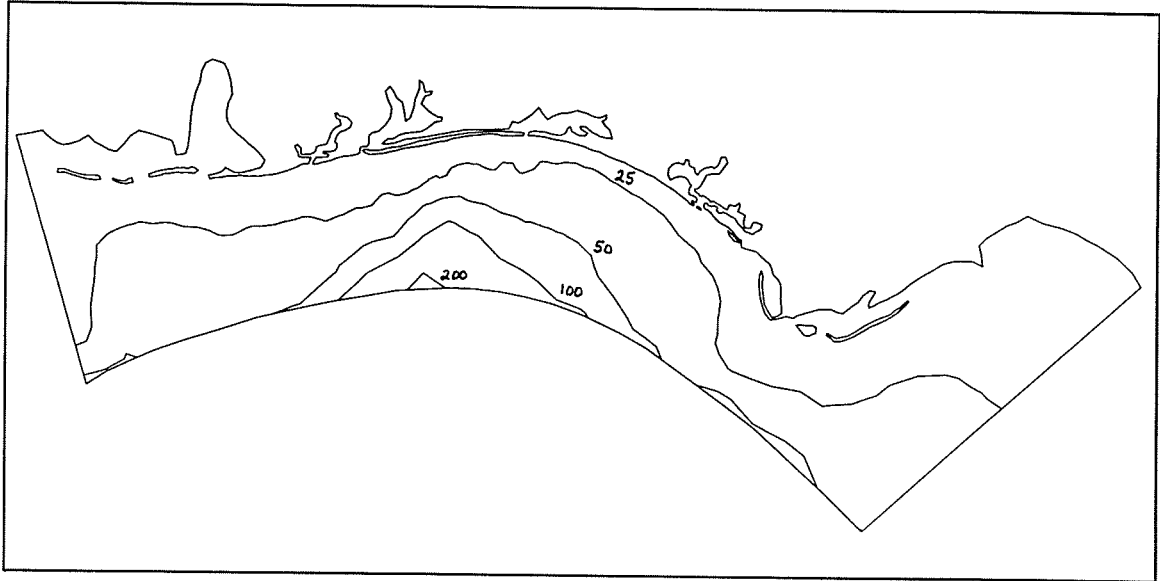


Figure 6. Bathymetry contours in increments of 25, 50, 100, and 200 m over the Florida coast domain

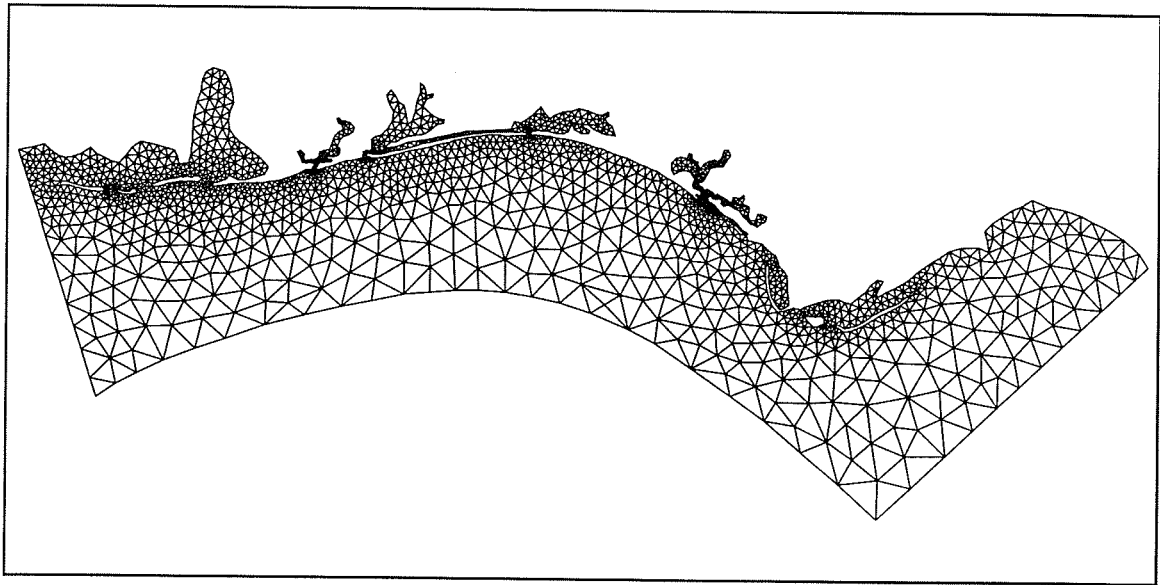


Figure 7. Florida coast domain discretization

<b>Table 1 Properties of the Computational Domains</b>									
Domain Name	Area (km <sup>2</sup> )	Maximum Bathymetry (m)	Domain Discretization		Approximate Grid Size		Resolution		
			Number of Nodes	Number of Elements	Maximum (degrees)	Minimum (degrees)	$\left(\frac{\lambda}{\Delta x}\right)_{max}$	$\left(\frac{\lambda}{\Delta x}\right)_{min}$	
East coast	8.3522x10 <sup>6</sup>	7,764.72	23,711	41,709	1.15	0.006	1,396.32	15.37	
Gulf of Mexico	1.4123x10 <sup>6</sup>	3,780.83	6,325	11,441	0.64	0.006	721.22	15.37	
Florida coast	3.6388x10 <sup>4</sup>	237.39	1,933	3,145	0.54	0.006	597.51	27.80	

## Storm Surge Simulations

Storm surge simulations are conducted over all three computational domains using the ADCIRC-2D code. A series of two simulations are run, one using wind and pressure forcing and the other applying wind and pressure forcing as well as an inverted barometer condition on the open boundary. In neither of these two sets of simulations is tidal forcing considered, either at the boundaries or on the interior of the domain. Identical model parameters for all simulations are selected so that comparison between the results for different domains is facilitated. The Florida coast and Gulf of Mexico domain simulations exhibit instabilities due to drying of elements, a feature not addressed by the ADCIRC model. Consequently, the model is run using only the nonlinear bottom friction option (i.e., the convective and finite amplitude terms are not included). A constant value of 0.003 is specified as the Manning friction coefficient,  $C_f$ , throughout all domains. Horizontal momentum diffusion is parameterized using an eddy viscosity formulation where the eddy viscosity coefficient is set equal to  $5 \text{ m}^2/\text{sec}$ . A GWCE parameter  $\tau_0$ , which represents the balance between the primitive continuity and wave equation portion of the GWCE, is defined equal to 0.001.

Simulations were spun up from homogeneous initial conditions using a 1-day ramp in time. Application of the hyperbolic ramp function reduces the excitation of nonphysical short wavelength frequencies. An identical ramp function of 1 day length is applied to the wind and pressure forcing as well as to an inverted barometer boundary condition when used. Actual simulations were run over 8.25 days, a period which includes the 1-day rampup. During the first 6 hr of the simulation, initial hurricane winds and pressure forcing are held stationary. Following these 6 hr, storm surge predictions begin at 1800 GMT, November 15, 1985, and continue for 8 days ending 1800 GMT, November 23, 1985. A time-step of 45 sec is used throughout the simulation period.

Elevation stations have been placed throughout all three domains. Locations of the elevation stations are identical in overlapping regions between the domains. Eleven stations are placed along the Florida Coast between St. Marks, FL, and the Mississippi Sound, and fifteen stations are located along the open ocean boundary of the Florida Coast domain. Around the remaining coastline of the Gulf of Mexico domain there are 16 elevation stations, and 12 more stations are placed along the open ocean boundary of the Gulf of Mexico domain. Finally, 11 additional elevation stations are specified in the east coast domain, one at Havana, Cuba, and the remaining 10 on the open ocean boundary. All 65 elevation station names and locations are shown in Figures 8, 9, and 10 for each computational domain.

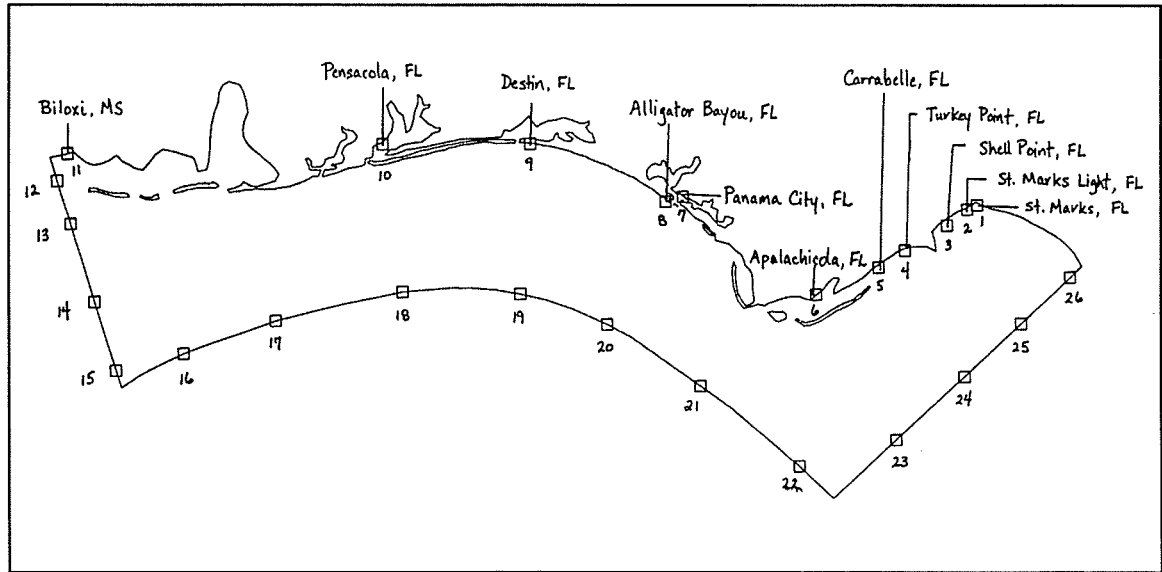


Figure 8. Names and locations of elevation stations in the Florida coast domain

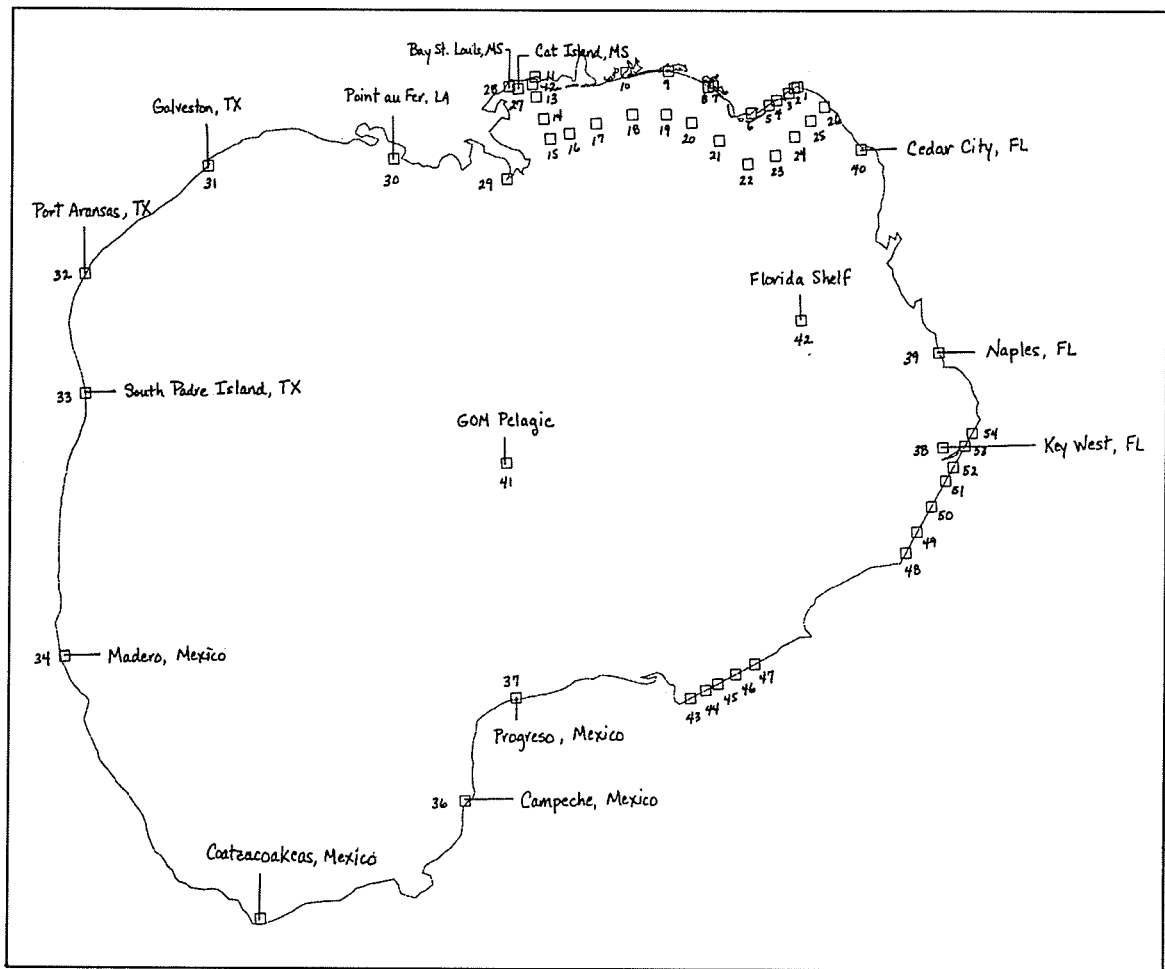


Figure 9. Names and locations of elevation stations in the Gulf of Mexico domain

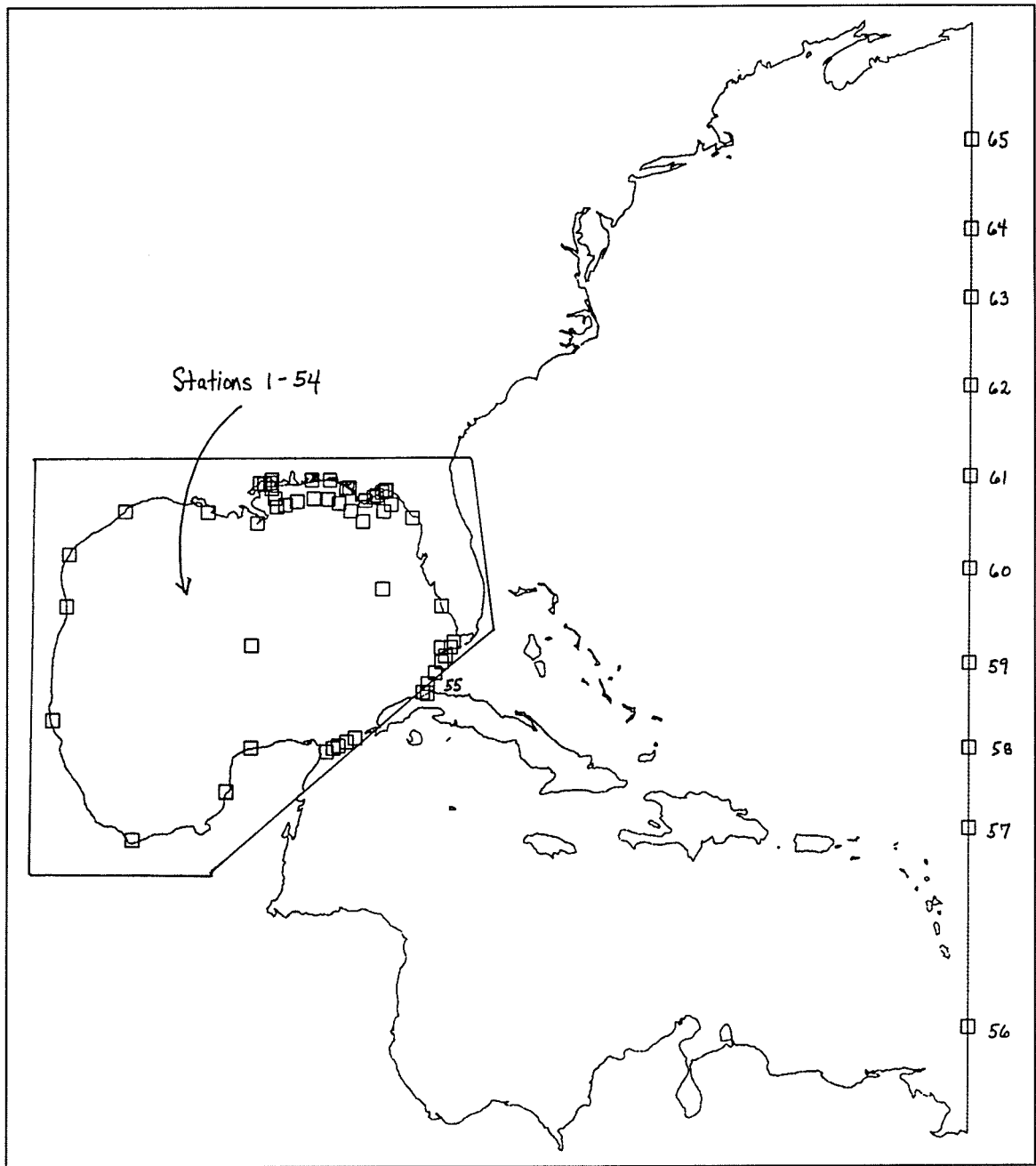
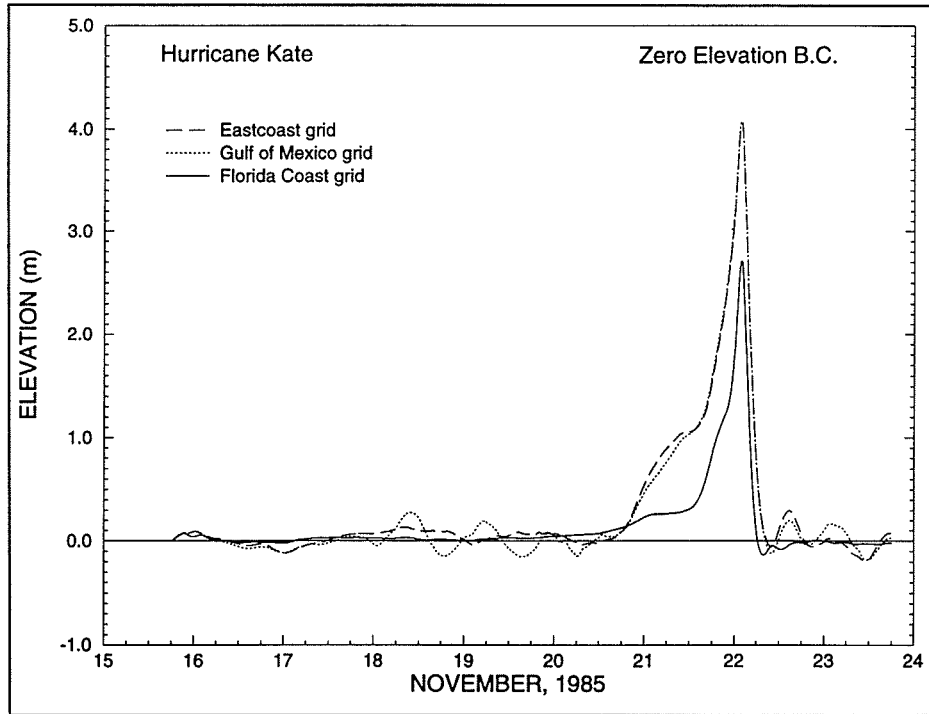


Figure 10. Names and locations of elevation stations in the east coast domain

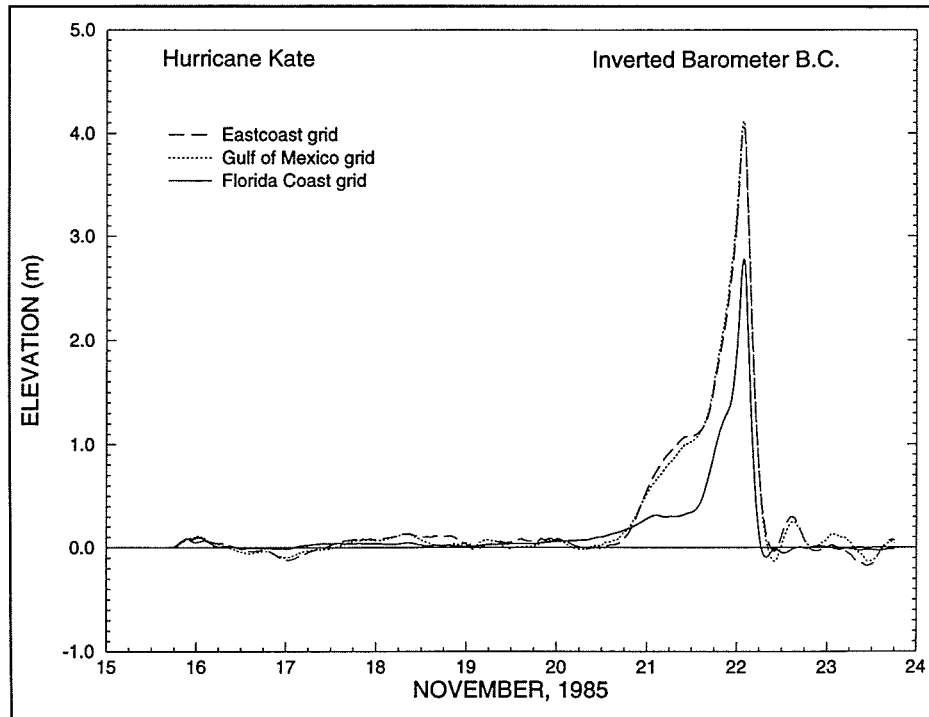


Two series of simulations are conducted, each implementing a different open boundary condition. In the first series of simulations, zero elevation is specified at all open boundary nodes in each domain. The second series of simulations applies an inverted barometer condition at all open boundary nodes. For these simulations, no calibration or tuning of parameters was performed, either in the weather model or in the hydrodynamic model.

Several observations arise from a comparison of storm surge predictions over each domain. The storm surge elevations predicted at St. Marks, Turkey Point, and Apalachicola, FL, are shown in Figures 11a, 12a, and 13a using a zero elevation open boundary condition and in Figures 11b, 12b, and 13b using an inverted barometer open boundary condition. Storm surge profiles at these stations are representative of conditions on the right-hand side of Hurricane Kate along the Florida coast. Clearly, the results point out the fact that the Florida coast domain significantly underpredicts peak storm surge and generally models the storm surge rather poorly as compared to the other domain results. For elevation stations near Panama City, Destin, and Pensacola, FL, storm surge profiles on the left-hand side of Hurricane Kate are presented in Figures 14a, 15a, and 16a for the zero elevation boundary condition and in Figures 14b, 15b, and 16b for the inverted barometer condition. When the hurricane winds come off the land, the Florida coast domain simulations exhibit excessive negative surges indicating that drying of coastal elements is occurring. Storm surge predictions from these simulations lead one to conclude that the Florida coast domain is an inadequate domain for simulating storm surge when compared with results from the two other domains considered here. Recall that the Florida coast and the Gulf of Mexico domains were cut from the east coast domain such that the discretization for all domains remain the same. Thus, any differences in storm surge prediction over the various domains are due strictly to the size of the domain and the boundary conditions used to drive the flow. Reiterating, a computational domain which covers only the continental shelf is inappropriate for storm surge prediction. This is related to the significant development of the storm surge which occurs as a hurricane moves over the rapid bathymetric changes of the continental slope and onto the continental shelf. Currently, most storm surge models still use continental shelf domains, clearly an inappropriate domain.

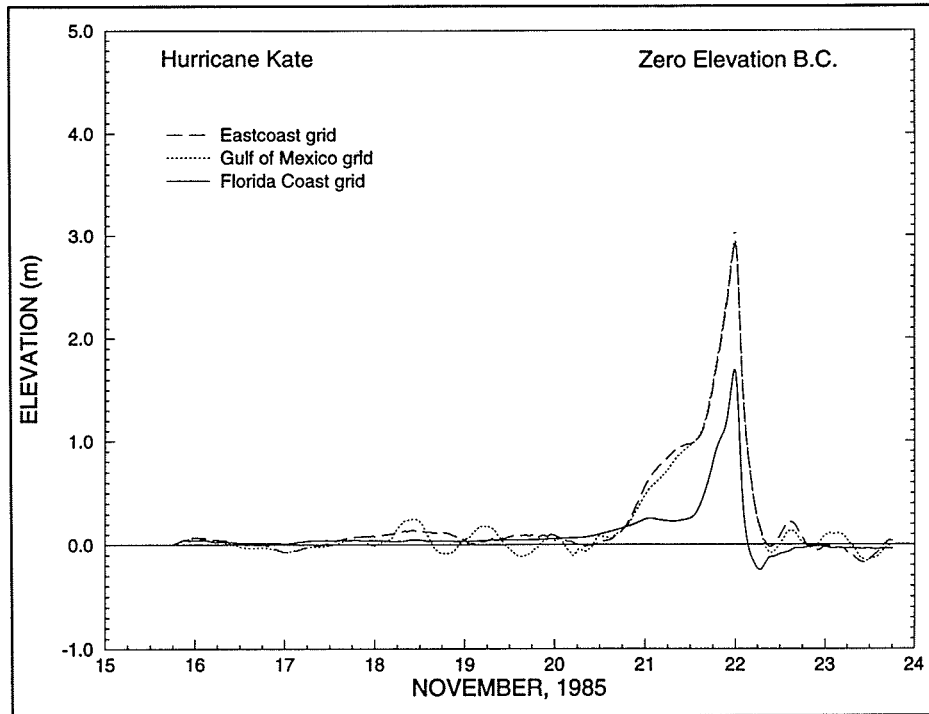


a. Zero elevation open boundary condition

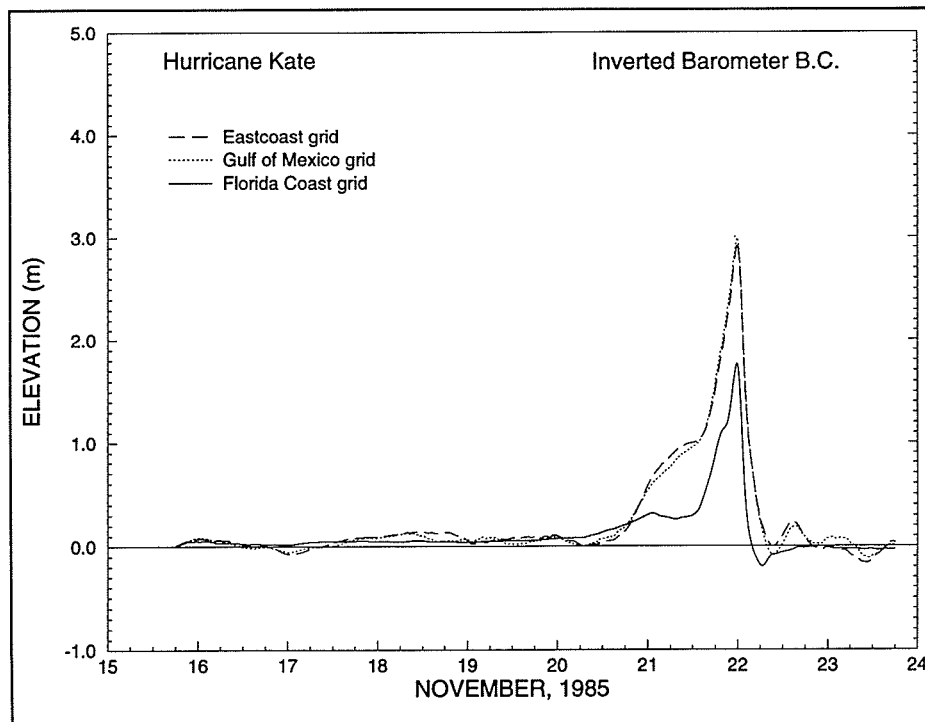


b. Inverted barometer open boundary condition

Figure 11. Computed storm surge for Hurricane Kate at St. Marks, Florida

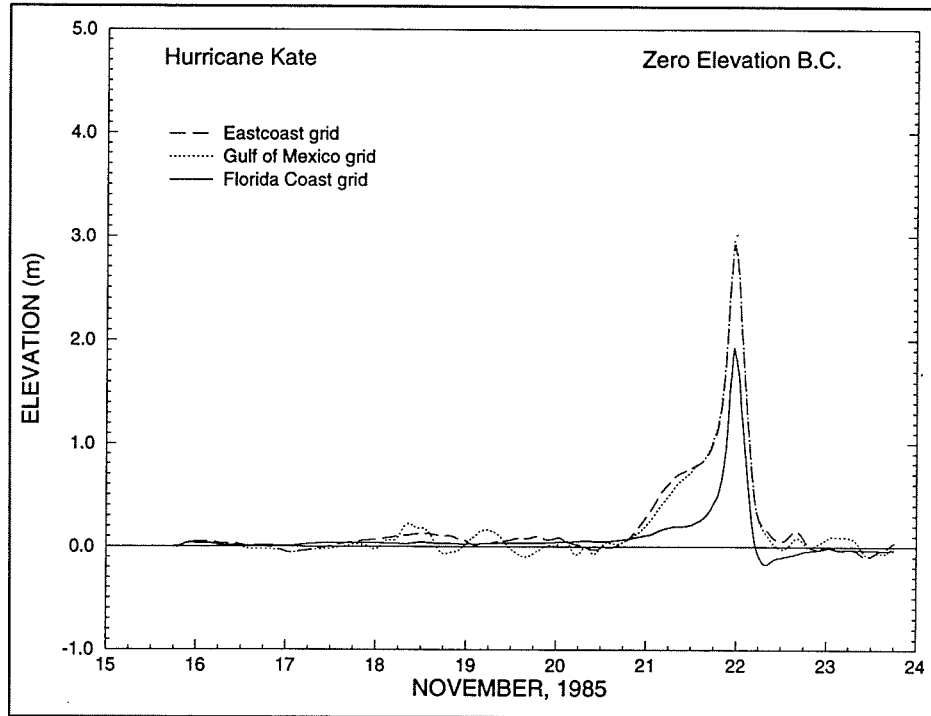


a. Zero elevation open boundary condition

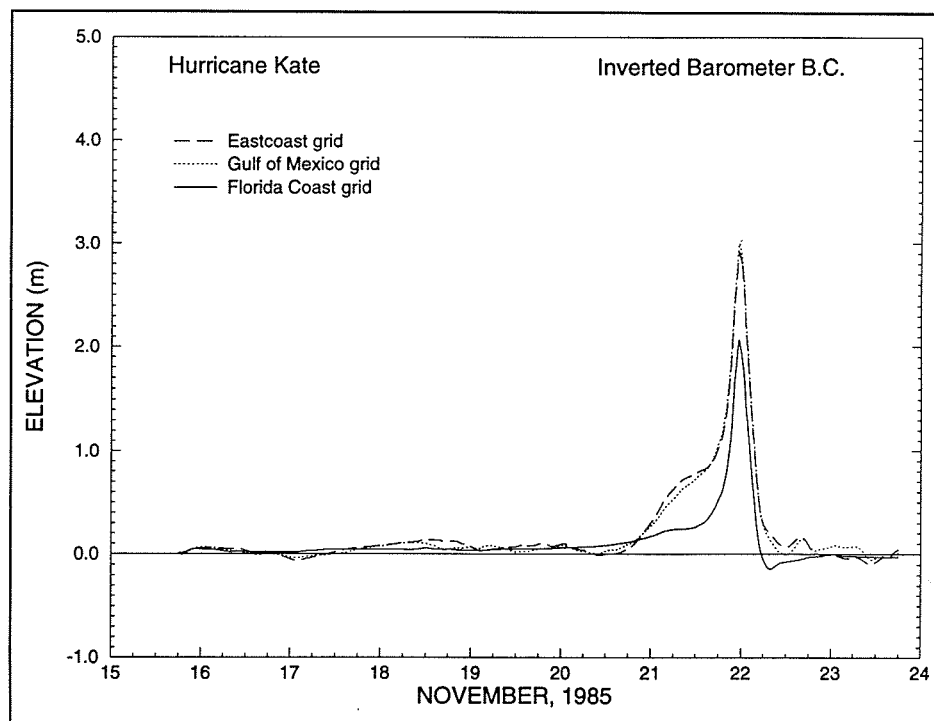


b. Inverted barometer open boundary condition

Figure 12. Computed storm surge for Hurricane Kate at Turkey Point, Florida

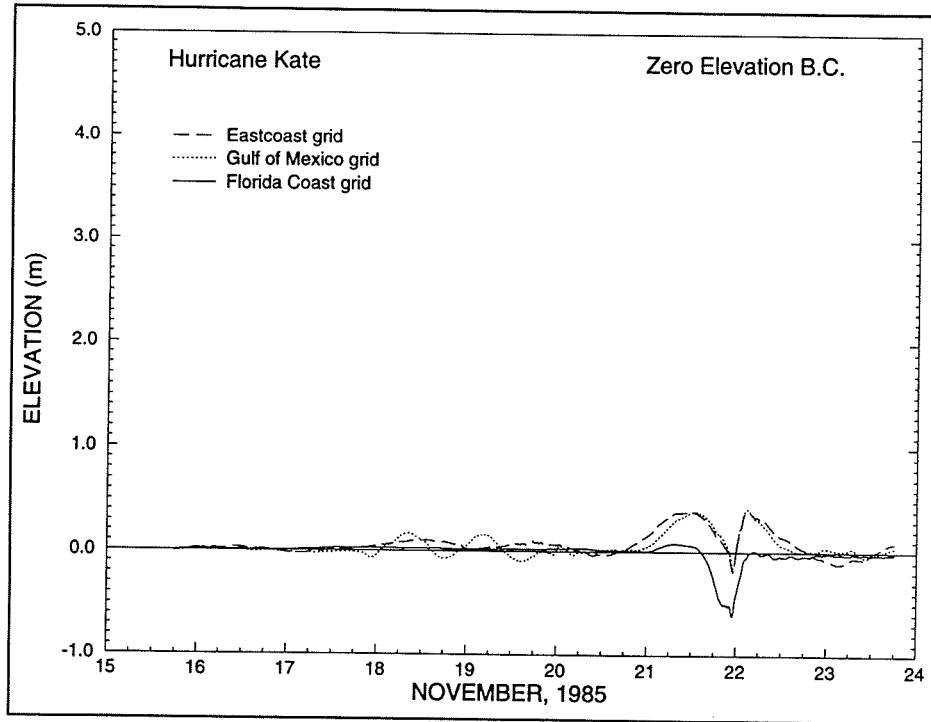


a. Zero elevation open boundary condition

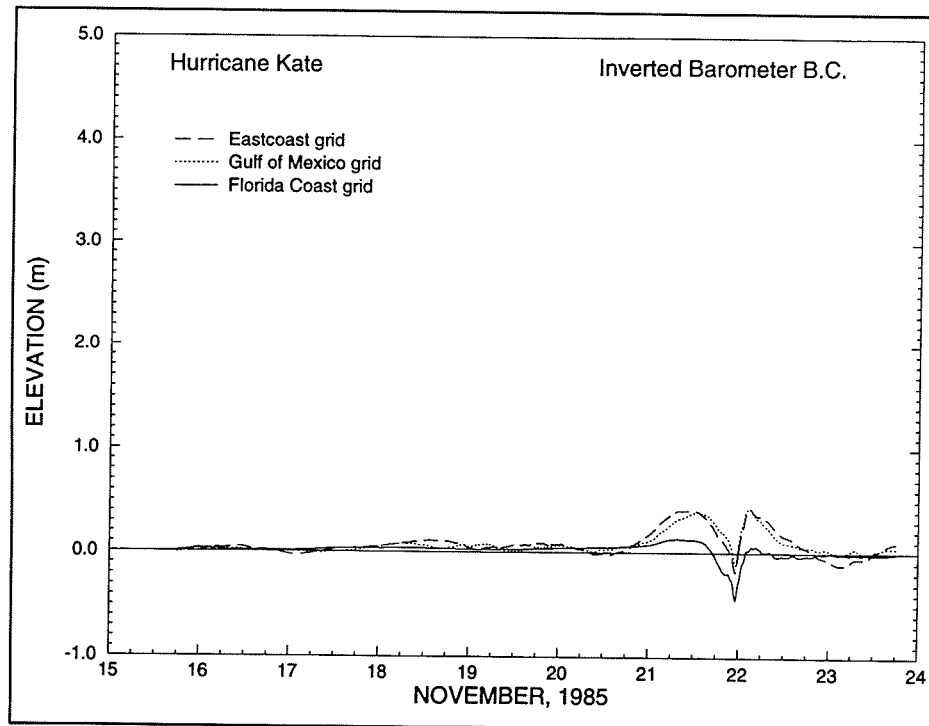


b. Inverted barometer open boundary condition

Figure 13. Computed storm surge for Hurricane Kate at Apalachicola, Florida

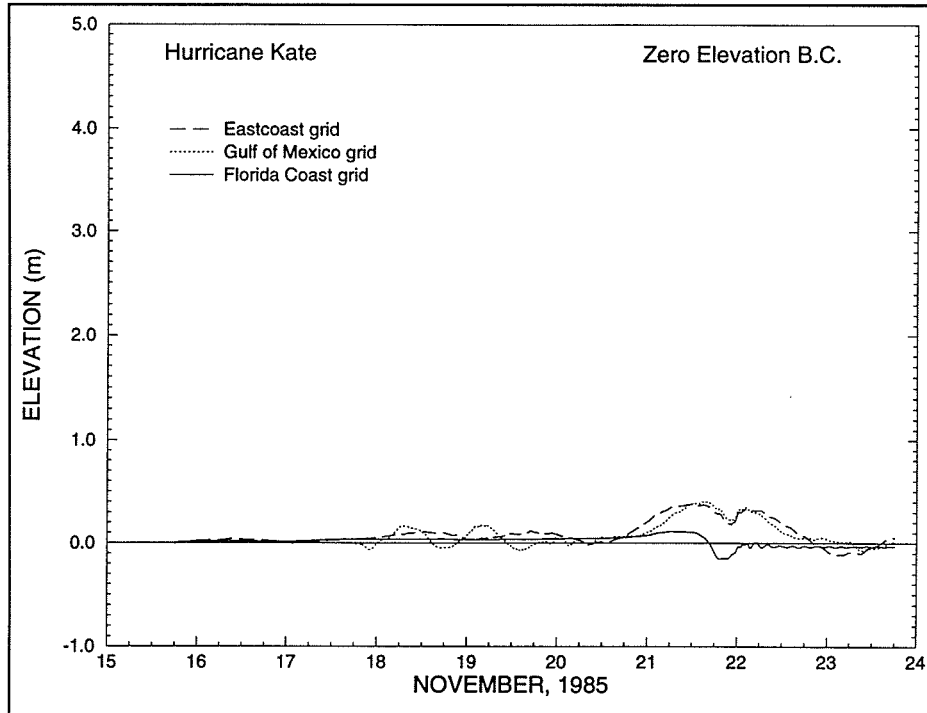


a. Zero elevation open boundary condition

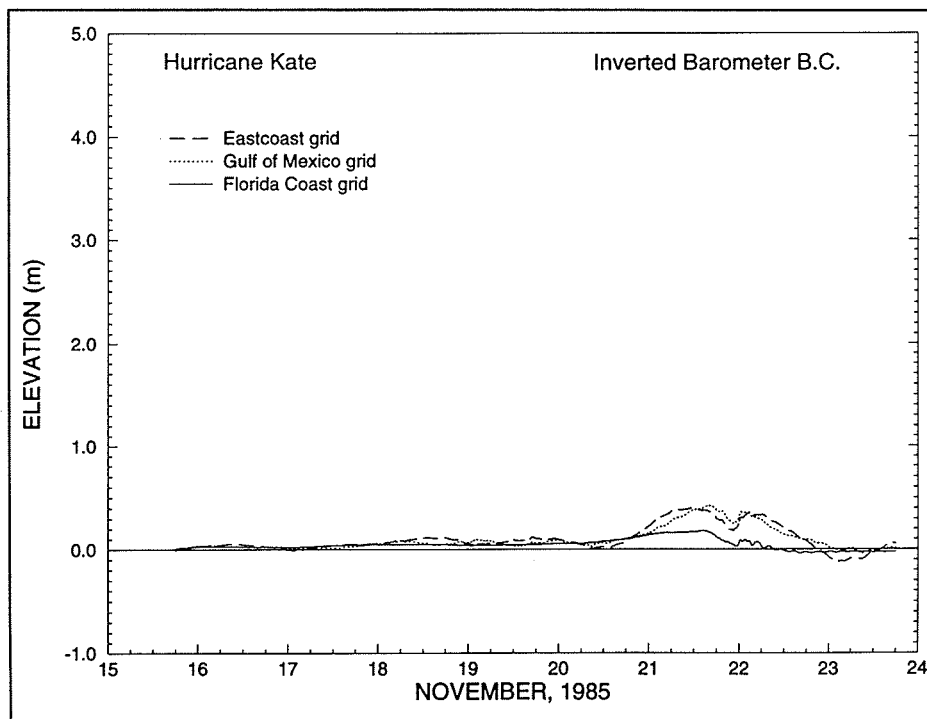


b. Inverted barometer open boundary condition

Figure 14. Computed storm surge for Hurricane Kate at Panama City, Florida

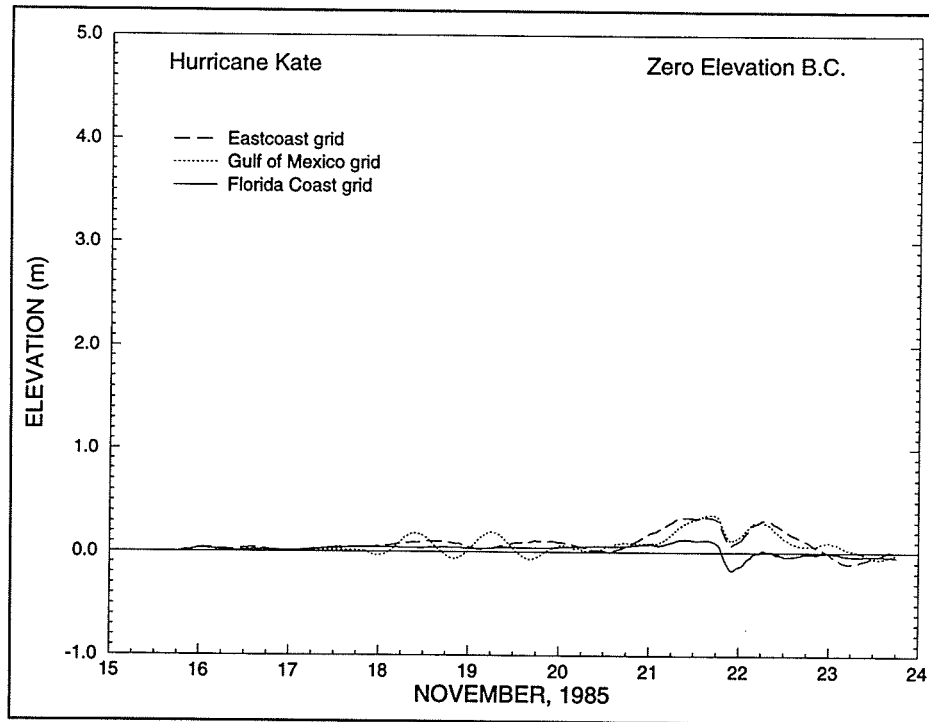


a. Zero elevation open boundary condition

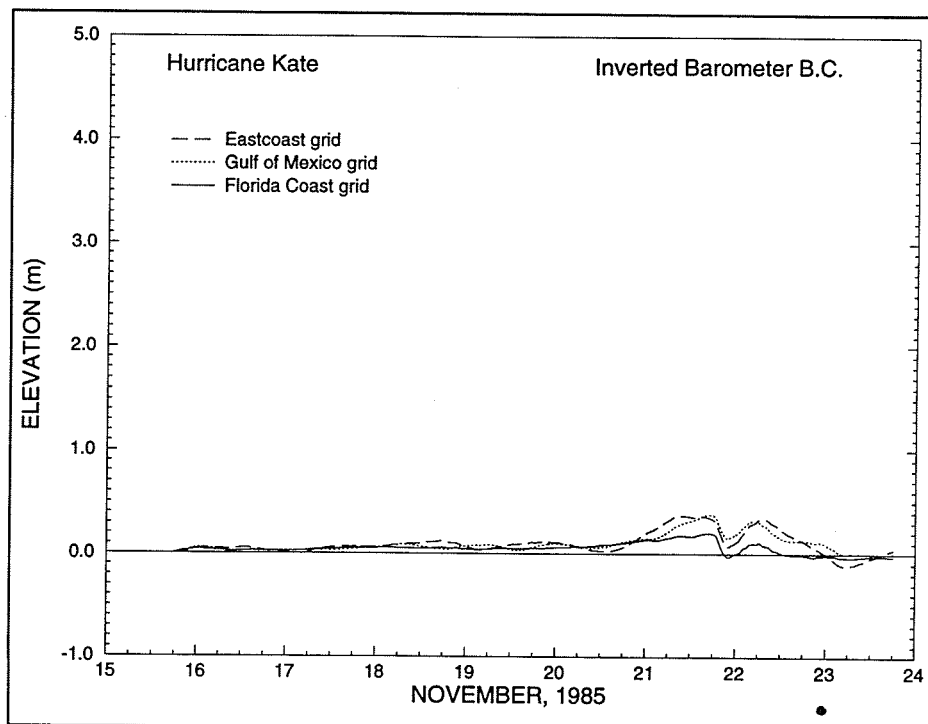


b. Inverted barometer open boundary condition

Figure 15. Computed storm surge for Hurricane Kate at Destin, Florida



a. Zero elevation open boundary condition



b. Inverted barometer open boundary condition

Figure 16. Computed storm surge for Hurricane Kate at Pensacola, Florida

Storm surge predictions for the Gulf of Mexico and east coast domains have peak surges which coincide in time and magnitude. However, oscillations plague the storm surge solution over the Gulf of Mexico domain as clearly indicated in all figures depicting storm surge associated with the zero elevation boundary condition. These oscillations are characteristic of the Gulf of Mexico whose resonant modes can be excited by the forcing functions, boundary conditions, and/or a specific domain as well as the domain discretization. When the inverted barometer boundary condition is used, the oscillations become less pronounced but still are evident. While in general the inverted barometer condition leads to an improvement in the storm surge predictions, an inverted barometer condition is not all that is needed for accurate storm surge prediction. Figures 17-19 compare inverted barometer values on the open ocean boundary of the Florida coast domain to storm surge elevations generated over the Gulf of Mexico and east coast domains. From these comparisons, it is obvious that an inverted barometer condition near the continental shelf break will grossly underestimate storm surge entering the domain. This is expected since the storm surge in shallow water is created by the interaction of both wind and pressure forcing with local bathymetry and coastal geometry. Over the east coast domain, the inverted barometer condition leads to minimal changes in storm surge elevation as shown by Figure 20, in which storm surge profiles for the zero elevation and inverted barometer boundary conditions are compared at St. Marks, FL. In the large domain model, changes of surface water elevation in the deep ocean are largely due to pressure deficits. These pressure deficits can be quite small in the deep ocean and thus surface water elevations specified at this deep ocean boundary have a minimal influence on storm surge generation in the near coastal region. The storm surge predictions shown in Figure 20 are evidence of the reduced effect of the deep ocean boundary conditions.

Storm surge predictions over three different-sized domains were compared and the largest, the east coast domain, was selected as the optimal computational domain. A large domain permits a realistic response of the coastal region to wind and pressure forcing. The generation and propagation of storm surge in a large domain is well represented because bathymetric changes in the continental slope and shelf region, complex coastal geometries, and the influence of adjacent basins are properly incorporated. In addition, a large domain has open boundaries in the deep ocean which are free from the complex interactions between coastal geometry, bathymetry, and wind and pressure forcing near or on the shelf. Specification of open boundary elevations in the deep ocean are thus simplified. Also, since the deep ocean boundary is far from the coastal region, elevations specified at this boundary have a minimal influence on coastal storm surge generation.



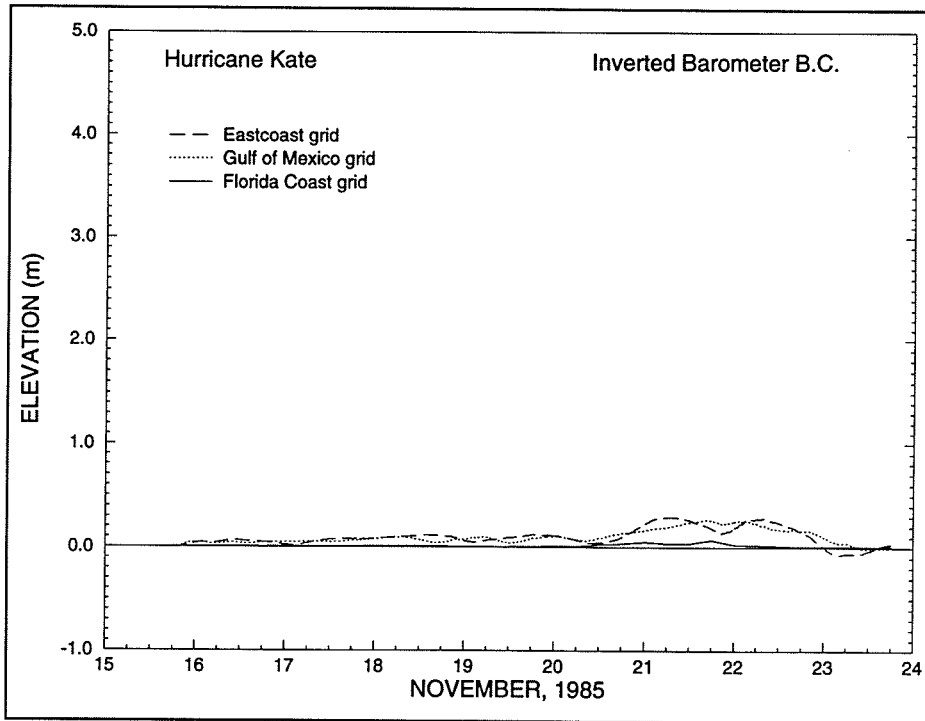


Figure 17. Comparison of computed storm surge for Hurricane Kate using an inverted barometer open boundary condition at Station 14 located on the Florida coast domain open boundary

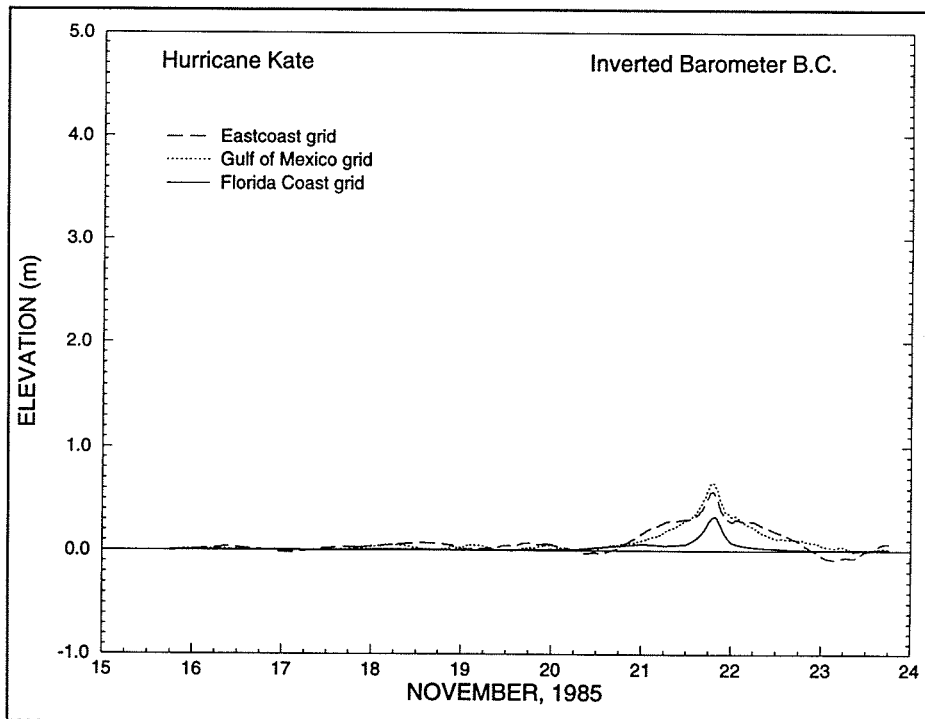


Figure 18. Comparison of computed storm surge for Hurricane Kate using an inverted barometer open boundary condition at Station 20 located on the Florida coast domain open boundary

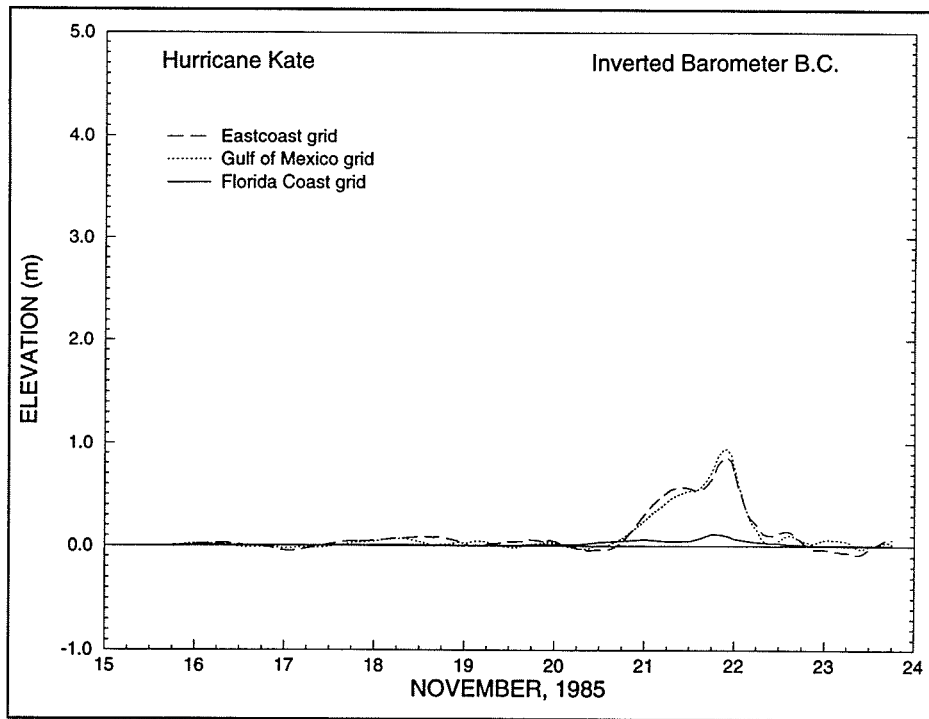


Figure 19. Comparison of computed storm surge for Hurricane Kate using an inverted barometer open boundary condition at Station 23 located on the Florida coast domain open boundary

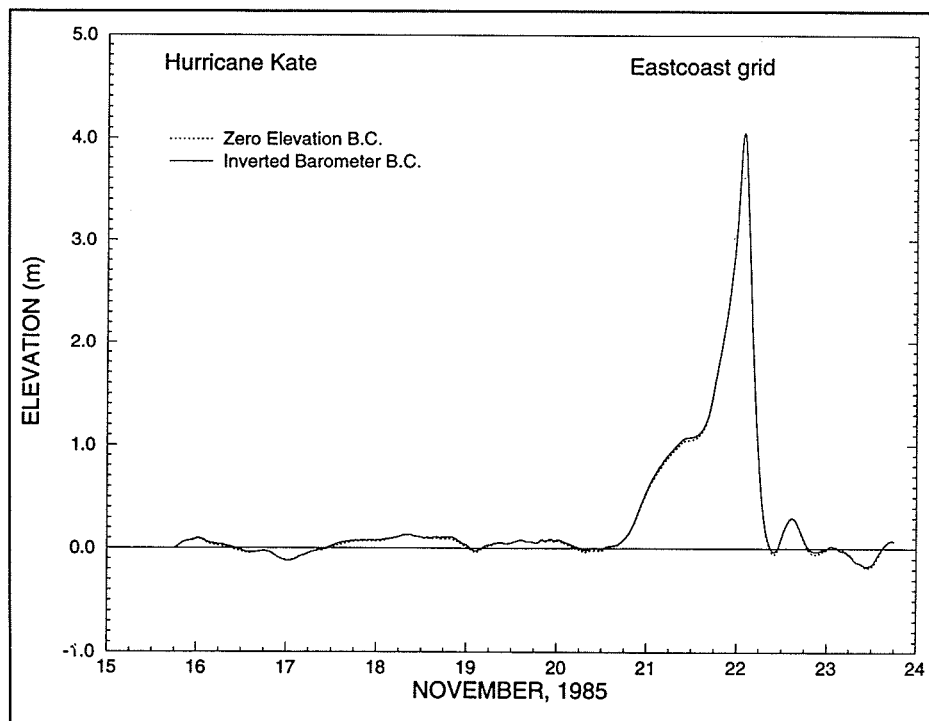


Figure 20. Comparison of computed storm surge for Hurricane Kate over the east coast domain using both a zero elevation and an inverted barometer open boundary condition at St. Marks, Florida

## 6 Comparison Between Computed and Observed Storm Surge Elevations Using a Large Domain

---

As a demonstration of the storm surge prediction capabilities of the ADCIRC code, Hurricane Kate is modeled. Computed storm surge profiles at eight elevation stations are compared to measured storm surge data for verification of the model results. From the computational domain comparisons, the east coast domain is selected as being the appropriate computational domain for the storm surge simulations.

The ADCIRC-2D model is run with all nonlinear options with the exception of the finite amplitude terms. These terms were not included in the formulation because of problems created by the drying of coastal areas due to the excessive wind speeds coming off the land on the left side of the hurricane. All other model parameters, including the time-step, remain as specified for the domain comparison simulations detailed in the previous section.

Another addition to the runs presented in the previous section is that tidal forcing is now included in the storm surge simulations. The tidal potential function is applied throughout the interior of the domain and tidal elevation forcing is specified along the open ocean boundary. Five tidal constituents,  $K_1$ ,  $O_1$ ,  $P_1$ ,  $M_2$ , and  $S_2$ , are considered both on the interior and at the open ocean boundary. Table 2 details the frequencies, nodal factors, equilibrium arguments, and Earth elasticity factors used for each constituent. The values of these tidal parameters are defined with reference to November 19, 1985, 0:00 GMT. Along the open ocean boundary, tidal elevations are obtained from Schwiderski's global model (Schwiderski 1979;1981a-g). For these simulations, the amplitude of the  $M_2$  tide, as reported by Schwiderski, is reduced by 10 percent, a correction in accordance with the error analysis of Westerink, Luetlich, and Scheffner (1993) as determined by their tidal model of the Western Atlantic Ocean.

Table 2 Tidal Potential Constants Used for Tidal and Storm Surge Simulations					
Constituent	Period (hr)	Potential Amplitude (m)	Earth Tide Reduction Factor	Nodal Factor	Equilibrium Argument (degrees)
$K_1$ luni-solar	23.934470	0.141565	0.736	1.086	321.3
$O_1$ principal lunar	25.819342	0.100514	0.695	1.140	271.35
$P_1$ principal solar	24.065890	0.046843	0.706	1.000	33.00
$M_2$ principal lunar	12.420601	0.242334	0.693	0.974	230.34
$S_2$ principal solar	12.000000	0.112841	0.693	1.000	0.00

Before proceeding to storm surge simulation, verification of the tidal responses throughout the east coast domain is undertaken. A 45-day simulation is conducted with a ramp-up period of 12 days. Results are recorded after 30 days of computation to ensure dissipation of free modes within the Gulf of Mexico and Caribbean as suggested by Westerink, Luettich, and Scheffner (1993). Computed tidal elevations at 77 stations, placed throughout the domain, are compared to measured data obtained at these same stations. Details regarding the location of the stations and the source of the tidal data can be found in Westerink, Luettich, and Scheffner (1993). Tidal predictions agree well with the measured data as seen in Figures 21-26. The slight downward adjustment of the  $M_2$  amplitude specified on the open boundary produces significantly improved tidal elevations at all stations as compared to those computed by Westerink, Luettich, and Scheffner (1993).

Storm surge predictions over the east coast domain include the tidal forcing just described as well as an inverted barometer condition on the open ocean boundary. The simulation begins with 36.75 days of tidal forcing before the hurricane enters the domain. Initial hurricane wind stress and pressure forcing are then held stationary for 6 hr. Following this period, storm surge computations continue for 8 days beginning at 1800 GMT, November 15, 1985, and ending 1800 GMT, November 23, 1985. Storm surge elevations are recorded every 3.75 min at eight elevation stations located along the Florida coastline from St. Marks, FL, to the Mississippi Sound. Measured storm surge values are available at these same locations. Comparisons of numerical storm surge predictions with measured storm surge elevations are presented in Figures 27-34. These results indicate that the storm surge from Hurricane Kate is well represented by the ADCIRC-2D model. Overprediction of the peak surge and the significant drop in surge at stations to the west of Apalachicola, FL, are both artifacts of the HURWIN model used to generate the wind stress forcing.

A severe limitation of the HURWIN wind model is its inability to account for frictional dissipation of the winds as a hurricane makes landfall. As winds rotate over land their magnitude remains high and subsequent drying of coastal regions occurs. This drying causes a large reduction in storm surge elevation, so much so, in fact, that significant negative storm surge values are recorded which are not in accordance with measured data. The HURWIN hurricane wind model does not account for dissipation of hurricane winds either in the open water prior to landfall or as winds rotate over land and come off the shore. Thus, the wind stress values, computed by the HURWIN model and used by the ADCIRC model, are generally too high in the region of hurricane landfall.

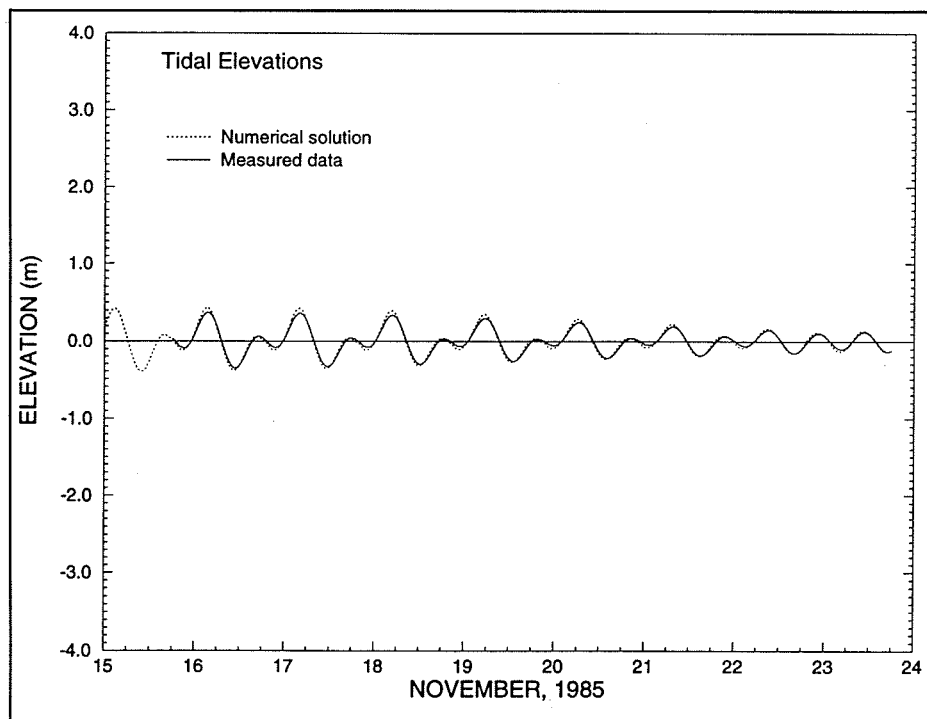


Figure 21. Comparison of computed and measured tidal elevations over the east coast domain at Key West, Florida

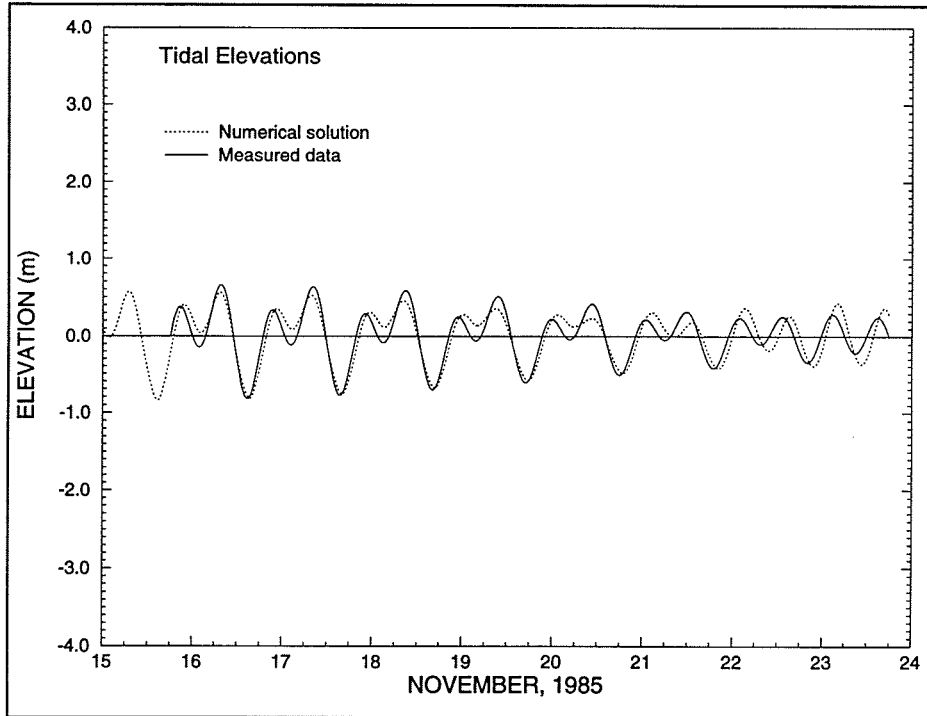


Figure 22. Comparison of computed and measured tidal elevations over the east coast domain at Cedar Key, Florida

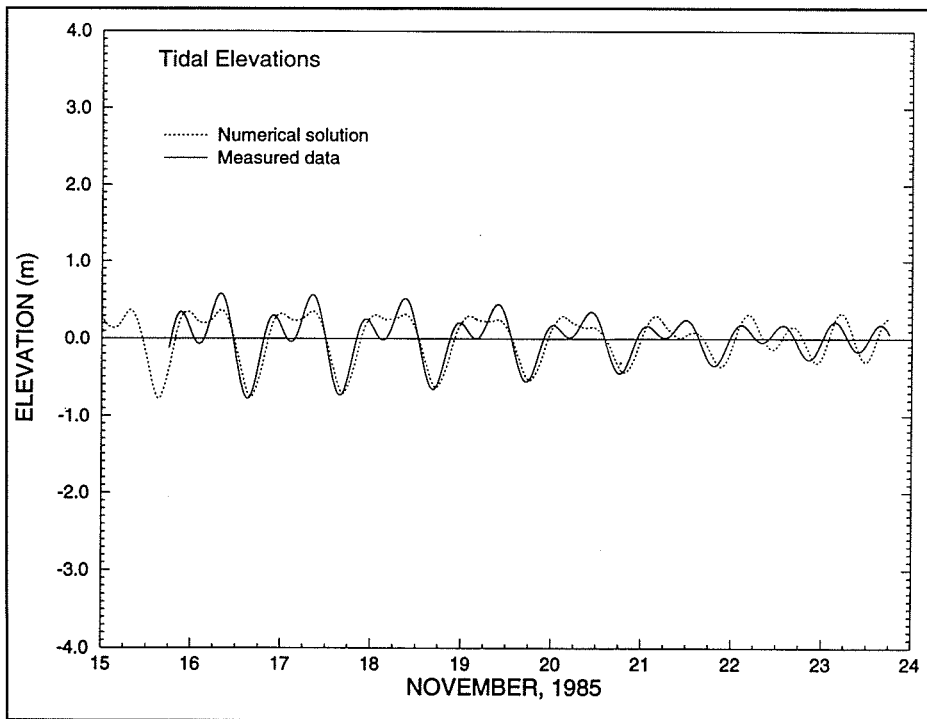


Figure 23. Comparison of computed and measured tidal elevations over the east coast domain at St. Marks Light, Florida

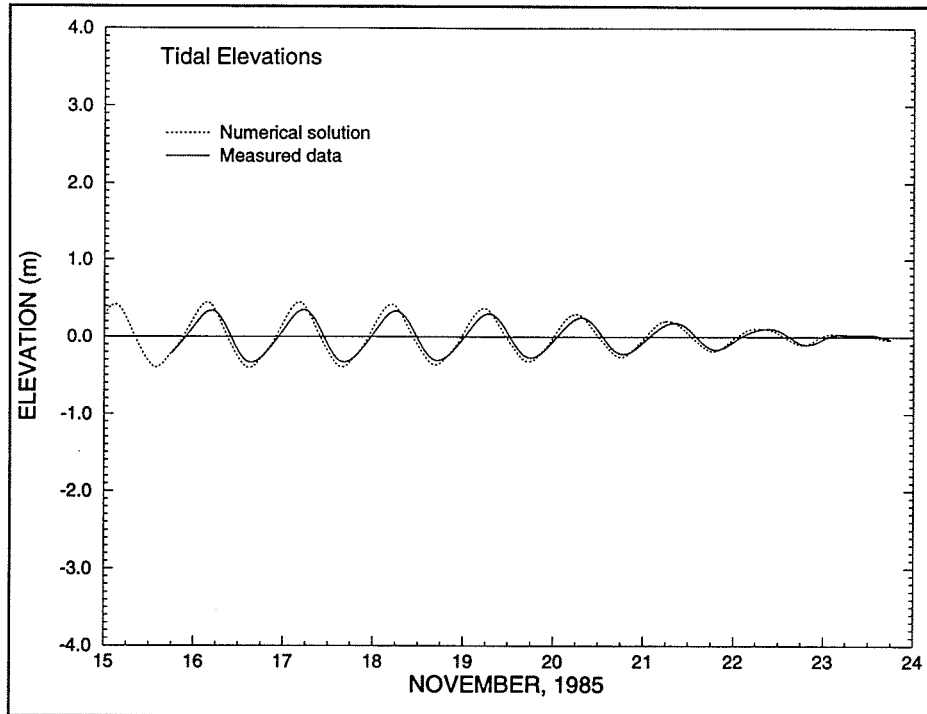


Figure 24. Comparison of computed and measured tidal elevations over the east coast domain at Alligator Bayou, Florida

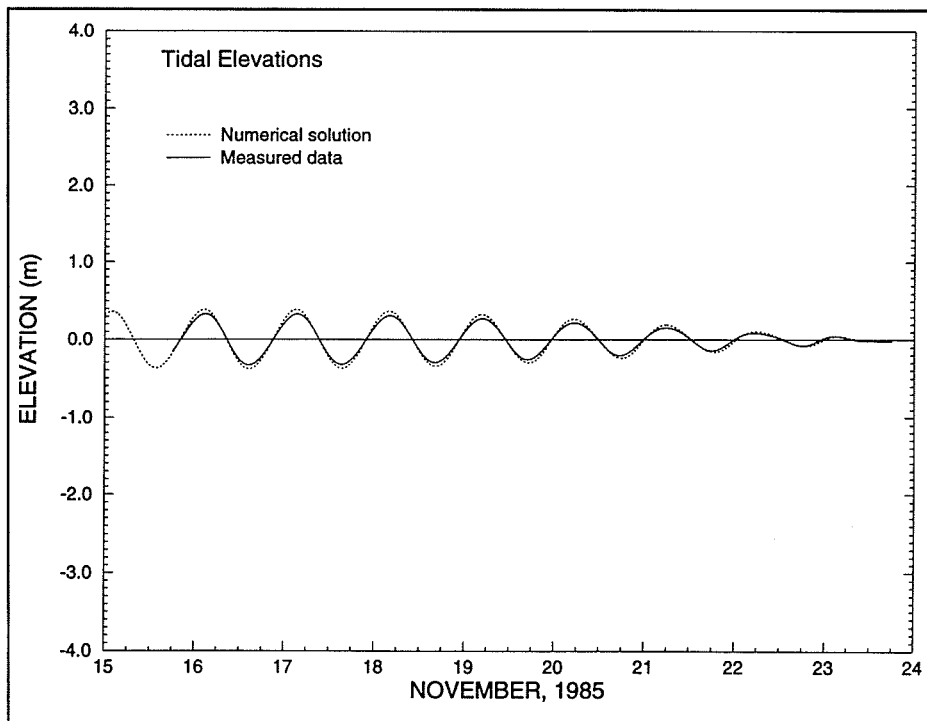


Figure 25. Comparison of computed and measured tidal elevations over the east coast domain at Southwest Pass, Louisiana

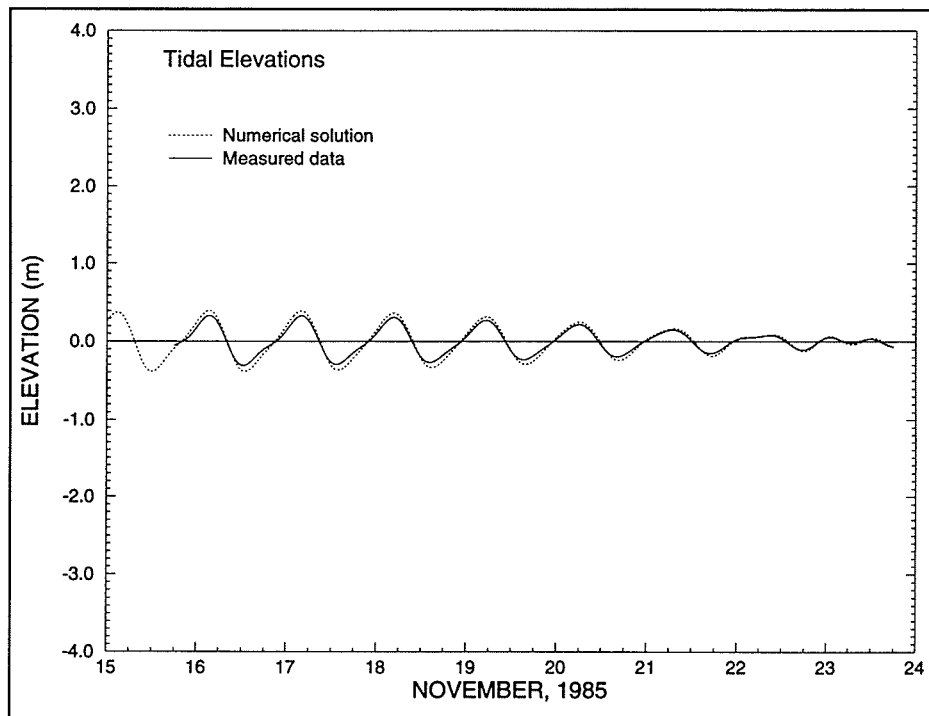


Figure 26. Comparison of computed and measured tidal elevations over the east coast domain at Western Florida Outer Shelf

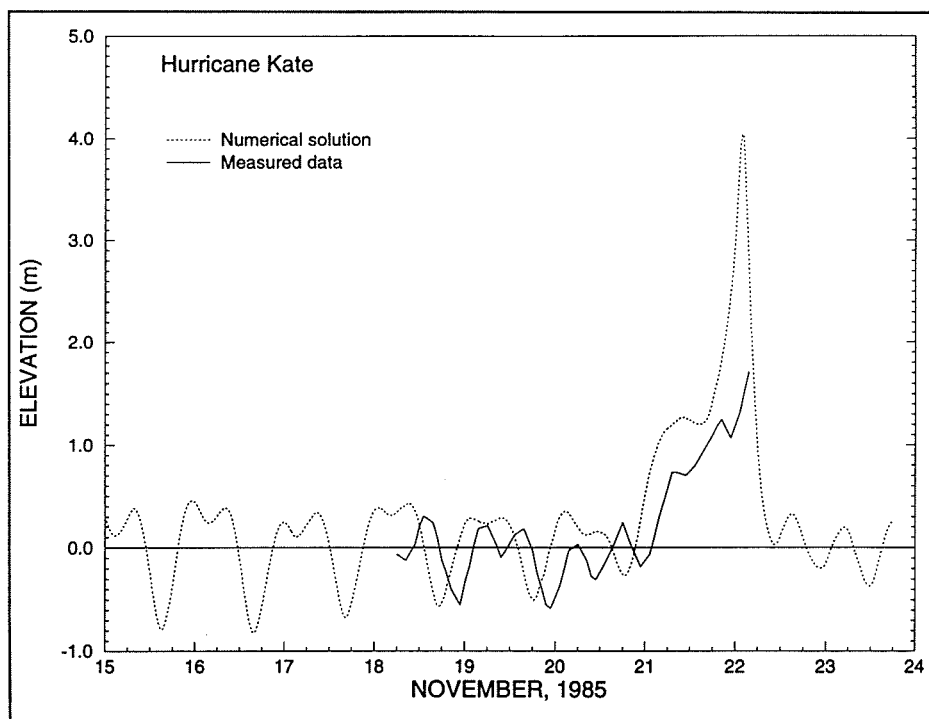


Figure 27. Comparison of computed and measured storm surge elevations for Hurricane Kate over the east coast domain at St. Marks, Florida



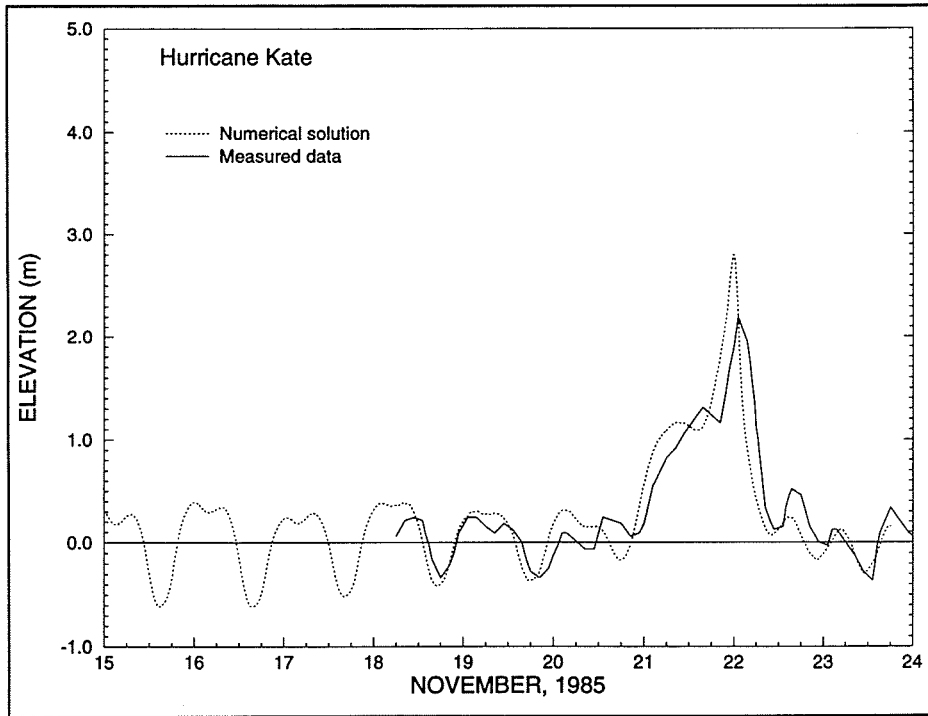


Figure 28. Comparison of computed and measured storm surge elevations for Hurricane Kate over the east coast domain at Turkey Point, Florida

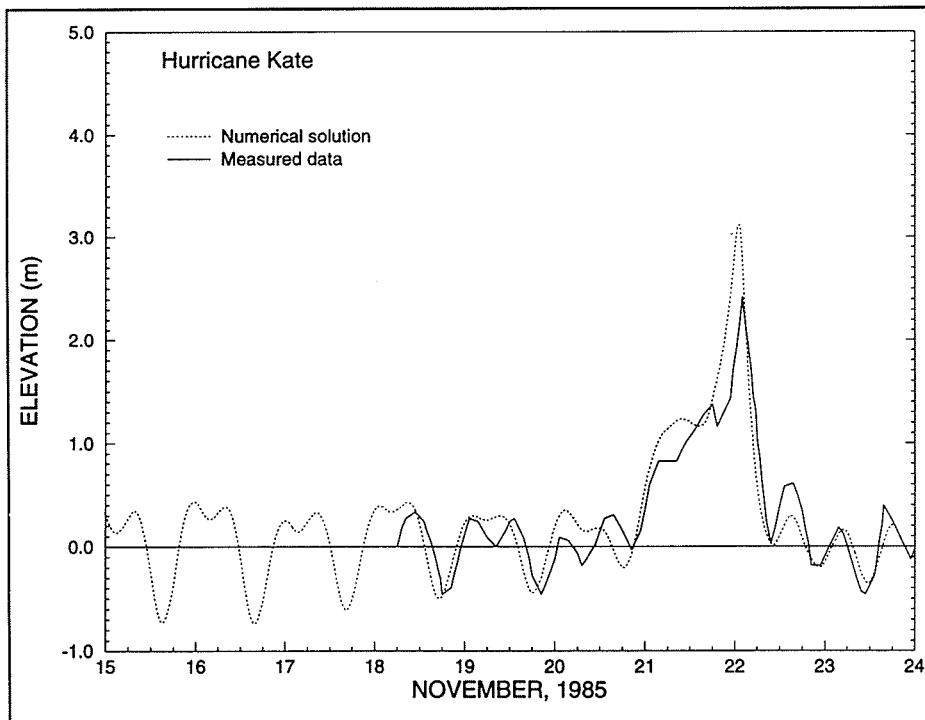


Figure 29. Comparison of computed and measured storm surge elevations for Hurricane Kate over the east coast domain at Shell Point, Florida

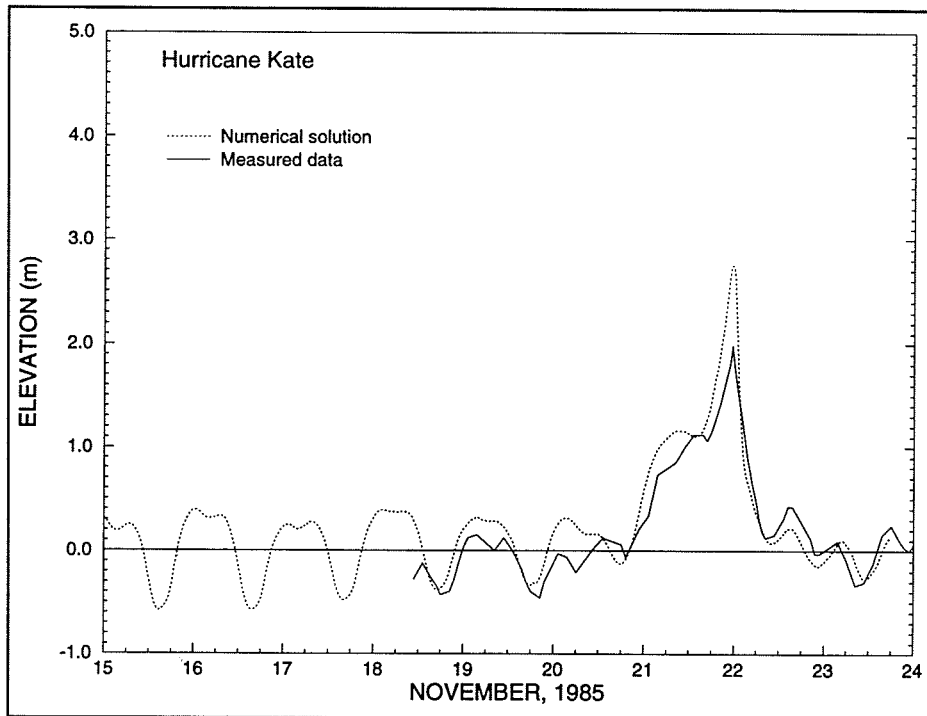


Figure 30. Comparison of computed and measured storm surge elevations for Hurricane Kate over the east coast domain at Carrabelle, Florida

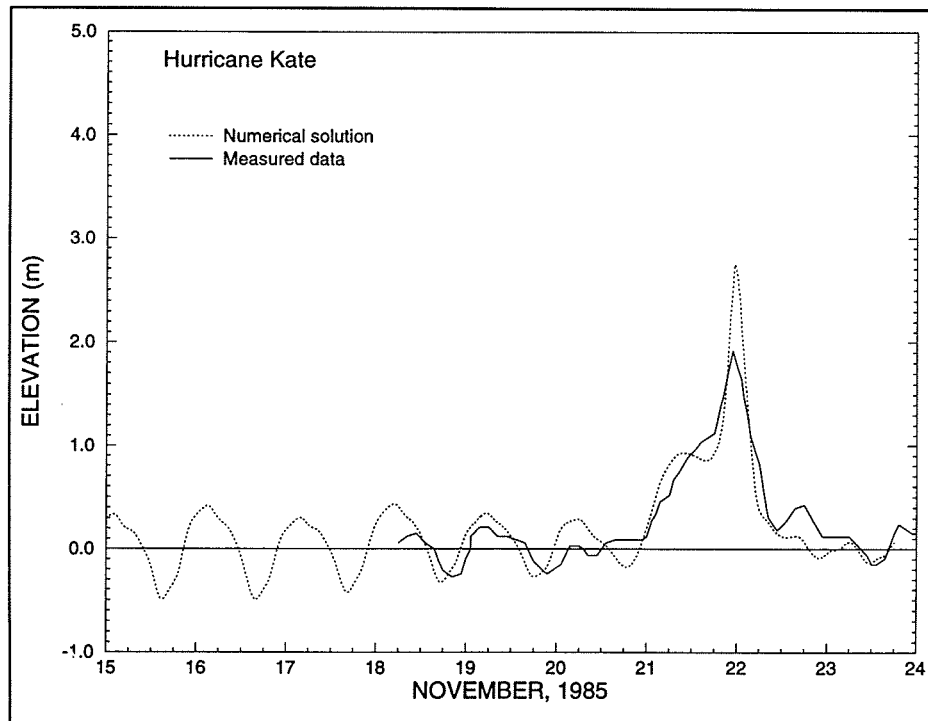


Figure 31. Comparison of computed and measured storm surge elevations for Hurricane Kate over the east coast domain at Apalachicola, Florida

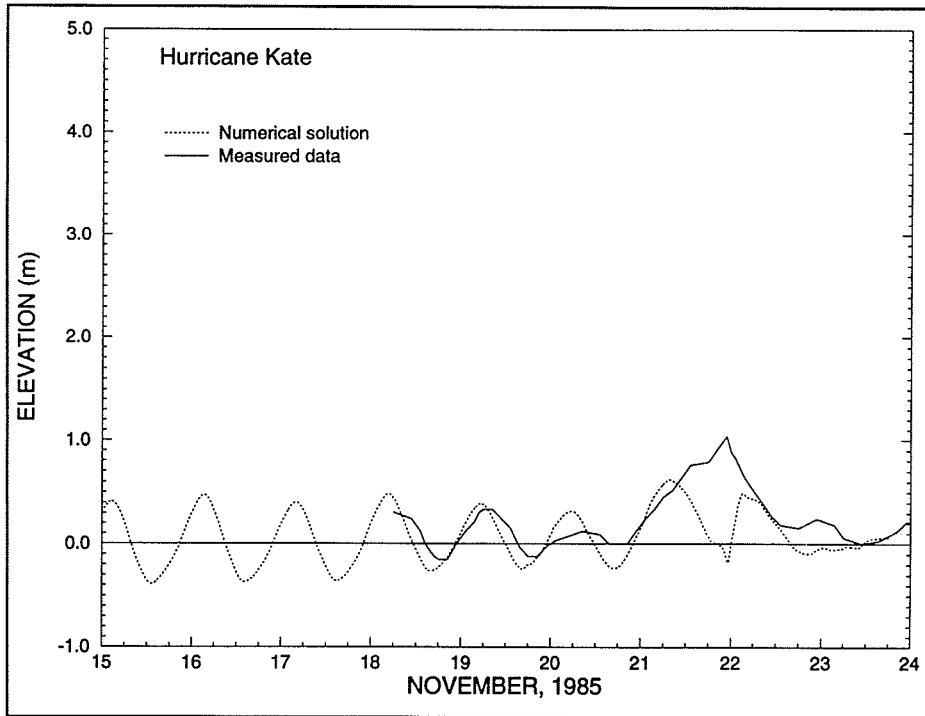


Figure 32. Comparison of computed and measured storm surge elevations for Hurricane Kate over the east coast domain at Panama City, Florida

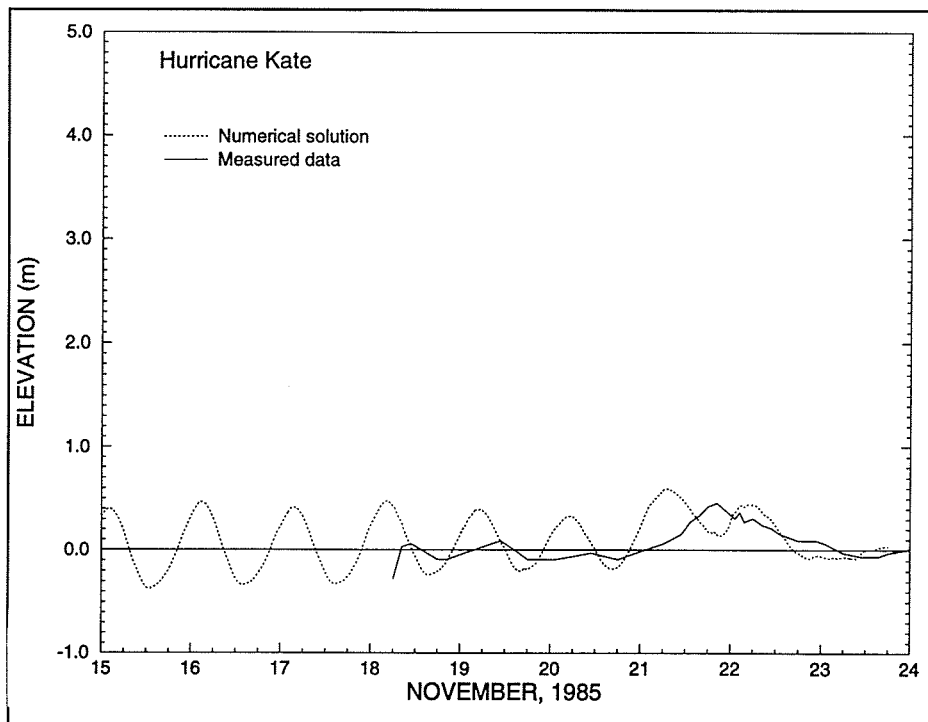


Figure 33. Comparison of computed and measured storm surge elevations for Hurricane Kate over the east coast domain at Destin, Florida

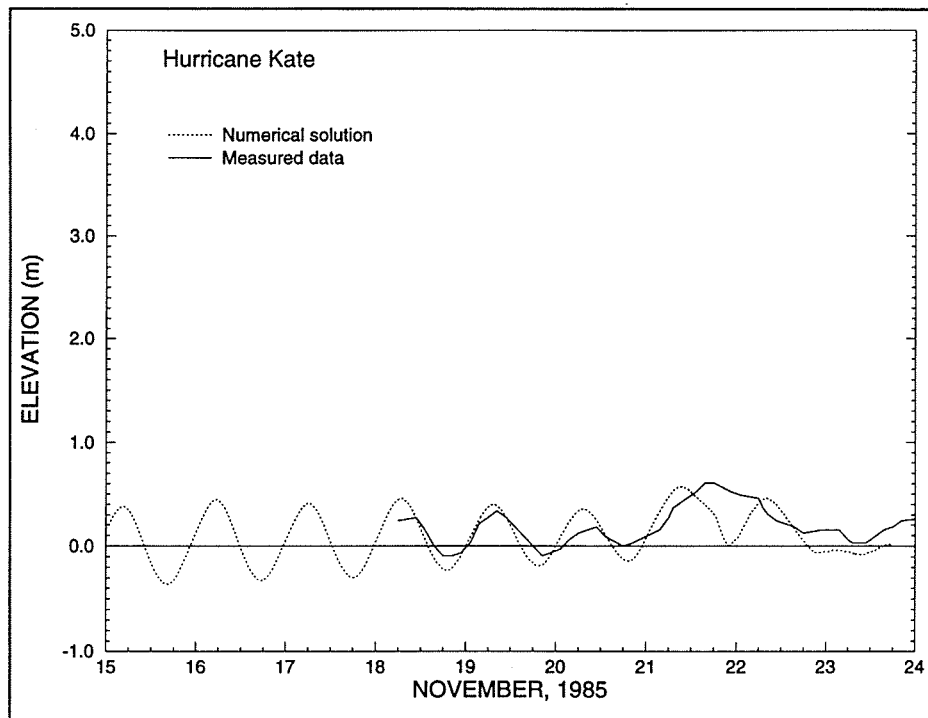


Figure 34. Comparison of computed and measured storm surge elevations for Hurricane Kate over the east coast domain at Pensacola, Florida

## 7 Conclusions

---

Most storm surge modeling efforts to date have used domains that are confined to the continental shelf. Little effort has been given to understanding the effect of domain size on storm surge predictions and the subsequent selection of an appropriate storm surge domain. In this report, storm surge calculations over three successively larger domains clearly illustrate that storm surge models restricted to the continental shelf severely underestimate the peak surge and do not reproduce coastal storm surge profiles in an acceptable fashion. Storm surge intensification results from the complex interactions between coastal geometry, bathymetry, and wind and pressure forcing as water is pushed up the continental slope and onto the shelf. This report demonstrates that these processes cannot be properly accounted for at the open boundaries of a shelf model. Thus, a storm surge model using a continental shelf domain is inappropriate.

Another size domain is one that covers the entire Gulf of Mexico. Solutions obtained for storm surge elevation over the Gulf of Mexico domain exhibit oscillatory behavior. Such oscillations are due to the existence of free modes in the Gulf of Mexico basin. These resonant modes in the Gulf of Mexico are well documented and can be easily excited by a number of factors: numerical discretization, forcing functions, and/or boundary conditions. Thus, storm surge elevations obtained over the Gulf of Mexico are considered unreliable due to the nature of the basin.

A very large domain, which includes the Western North Atlantic Ocean, the Gulf of Mexico, and the Caribbean, is found to be ideal. A hurricane can progress through the domain generating and propagating storm surge in a natural and realistic fashion. The inclusion of basins adjacent to the coastal region allows all wavelengths associated with storm surge to propagate through the domain and onto the continental shelf where development of storm surge is most critical. Factors that affect storm surge generation and propagation, such as bathymetric changes in the continental slope and shelf region, complex coastal geometries, and wind and pressure forcing, are all properly incorporated into a large domain model. Another advantage is that the open boundaries of a large domain lie in the deep ocean and are far from the intricate processes occurring in the continental shelf region. In the deep ocean, changes in the surface water elevation are largely due to pressure deficits whereas on the continental shelf both pressure and wind forcing are also

important. An inverted barometer condition can be easily and appropriately specified for the deep ocean boundary. Additionally, tidal elevations at the open boundary in a large domain model are readily extracted from global tidal models. Again, any errors due to the erroneous specification of boundary forcing are reduced in a large domain model because the open ocean boundary is located quite far from the coastal region of interest. For all of these reasons a large domain whose open boundary lies in the deep ocean is optimal for storm surge prediction.

The finite element formulation used in the ADCIRC hydrodynamic model facilitates use of a large computational domain. Flexibility of the finite element method leads to easy incorporation of coastline detail and nodal densities which can range from three to four orders of magnitude. A wide variation in nodal density arises due to significant refinement in coastal areas and in regions of rapid bathymetric changes where storm surge generation is important and subsequent coarse discretizations in the deep ocean where processes occur more gradually and are of less interest. The efficiency of the finite element method leads to a discrete problem, associated with the large domain, which remains well within computational limits.

Despite the more realistic theoretical basis of the HURWIN model, the model does not represent the processes associated with a hurricane making landfall. Frictional dissipation of the winds as a hurricane makes landfall is not addressed in either the open water prior to landfall or for winds that rotate over land and come off the shore. The artificially high magnitude of the wind field leads to overprediction of peak surges and drying in coastal regions, features not supported by the measurement data. Storm surge predictions over the large domain can be improved by incorporating into the wind model the dissipative processes involved when a hurricane makes landfall.

# References

---

- Al-Rabeh, A.H., Eunay, N., and Cekirge, H.M. (1990). "A hydrodynamic model for wind driven and tidal circulation in the Arabian Gulf," *Applied Mathematical Modelling* 14, 410-19.
- Bungapong, M., Reid, R.O., and Whitaker, R.E. (1985). "An investigation of hurricane-induced forerunner surge in the Gulf of Mexico," Technical Report CERC-85-5, U.S. Army Engineer Waterways Experiment Station, Vicksburg, MS.
- Cardone, V.J., Greenwood, C.V., and Greenwood, J.A. (1992). "Unified program for the specification of hurricane boundary layer winds over surfaces of specified roughness," Contract Report CERC-92-1, U.S. Army Engineer Waterways Experiment Station, Vicksburg, MS.
- Chow, S. (1971). "A study of the wind field in the planetary boundary layer of a moving tropical cyclone," M.S. thesis, New York University, New York.
- Dendrou, S.A., Moore, C.I., and Myers, V.A. (1985). "Application of storm surge modeling to coastal flood rate determinations," *Marine Science Technology Journal* 19, 42-49.
- Dube, S.K., Sinha, P.C., and Roy, G.D. (1986). "Numerical simulation of storm surges in Bangladesh using a bay-river model," *Coastal Engineering* 10.
- Flather, R.A. (1984). "A numerical model investigation of the storm surge of 31 January and 1 February 1953 in the North Sea," *Quarterly Journal of the Royal Meteorological Society* 110, 591-612.
- \_\_\_\_\_. (1988). "A numerical model investigation of tides and diurnal-period continental shelf waves along Vancouver Island," *J. of Physical Oceanography* 18, 115-39.
- Foreman, M.G.G. (1983). "An analysis of the wave equation model for finite element tidal comparisons," *Journal of Computational Physics* 52, 290-312.

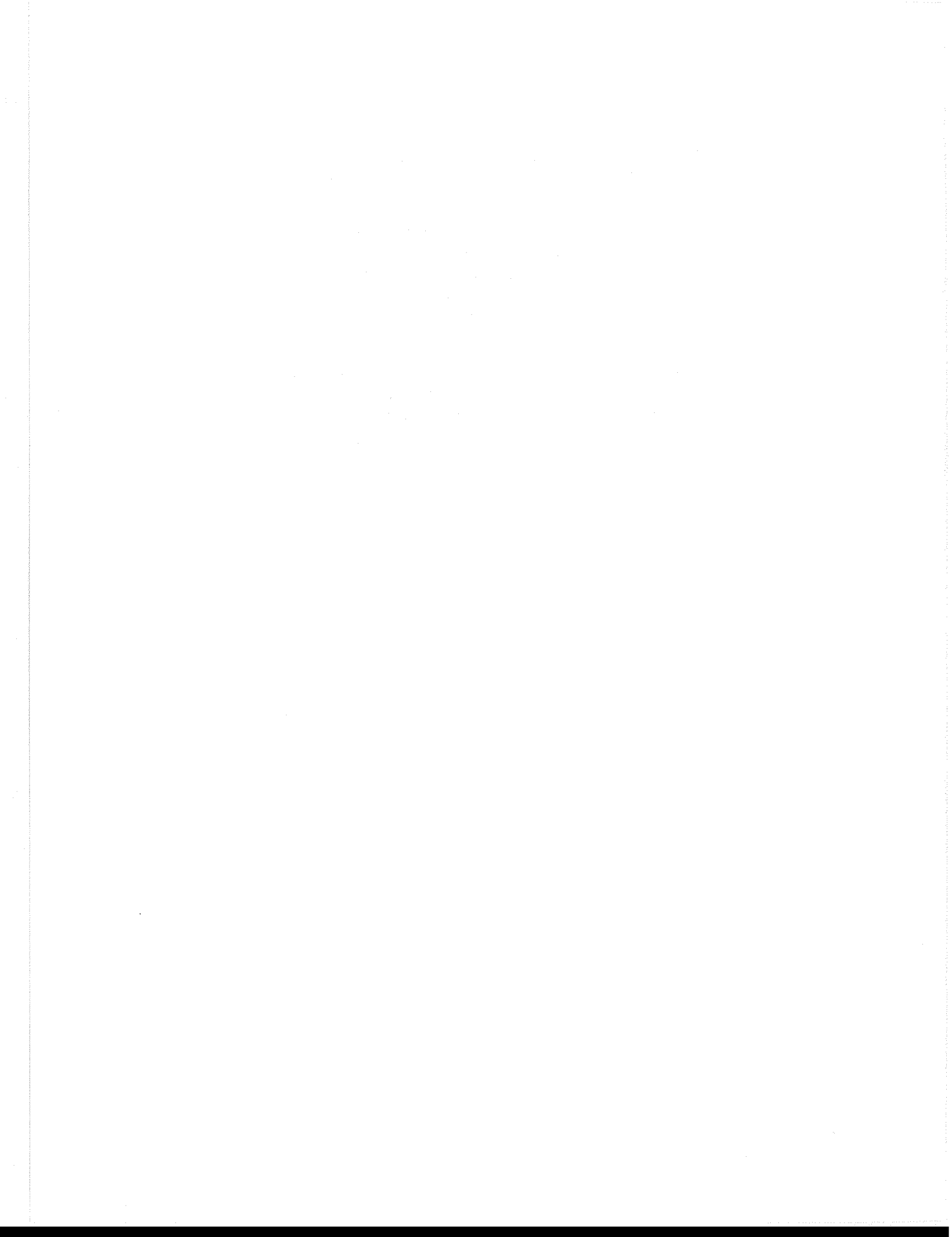
- Foreman, M.G.G. (1988). "A comparison of tidal models for the Southwest Coast of Vancouver Island." *Proceedings of the VII International Conference on Computational Methods in Water Resources*, held in Cambridge, MA, Elsevier, New York.
- Garcia, A.W. and Hegge, W.S. (1987). "Hurricane Kate storm surge data, Report 5," Technical Report CERC-87-12, U.S. Army Engineer Waterways Experiment Station, Vicksburg, MS.
- Garratt, J.R. (1977). "Review of drag coefficients over oceans and continents," *Monthly Weather Review* 105, 915-29.
- Gray, W.G. (1982). "Some inadequacies of finite element models as simulators of two-dimensional circulation," *Advances in Water Resources* 5, 171-77.
- \_\_\_\_\_. (1989). "A finite element study of tidal flow data for the North Sea and English Channel," *Advances in Water Resources* 12, 143-54.
- Hearn, C.J. and Holloway, P.E. (1990). "A three-dimensional barotropic model of the response of the Australian North West Shelf to tropical cyclones," *Journal of Physical Oceanography* 20, 60-80.
- Hendershott, M.C. (1981). "Long waves and ocean tides." *Evolution of physical oceanography*. B.A. Warren and C. Wunsch, ed., MIT Press, Cambridge, MA, 292-341.
- Hubbert, G.D., Leslie, L.M., and Manton, M.J. (1990). "A storm surge model for the Australian Region," *Quarterly Journal of the Royal Meteorological Society* 116, 1005-20.
- Jarvinen, B.R. and Lawrence, M.B. (1985). "An evaluation of the SLOSH storm-surge model," *Bulletin of American Meteorological Society* 11, 1408-11.
- Jelenianski, C.P. (1979). "Tropical storm surge forecasting in the National Weather Service." *ASCE Proceedings of the Engineering Foundation Conference on Improved Hydrologic Forecasting, Why and How?* Pacific Grove, CA, March 25-30, 65-75.
- Johns, B., Dube, S.K., Mohanty, U.C., and Rao, A.D. (1983a). "Simulation of storm surges using a three-dimensional numerical model: An application to the 1977 Andhra Cyclone," *Quarterly Journal of the Royal Meteorological Society* 109, 211-24.
- \_\_\_\_\_. (1983b). "On the effect of bathymetry in numerical storm surge simulation experiments," *Computers and Fluids* 11, 161-74.



- Kinnmark, I.P.E. (1984). "The shallow water wave equations: Formulation, analysis and application," Ph.D. diss., Department of Civil Engineering, Princeton University.
- Kolar, R.L., Gray, W.G., Westerink, J.J., and Luettich, R.A. (1994). "Shallow water modeling in spherical coordinates: Equation formulation, numerical implementation, and application," *Journal of Hydraulic Research* 32(1), 3-24.
- Lardner, R.W. and Cekirge, H.M. (1988). "A new algorithm for three-dimensional tidal and storm surge computations," *Applied Mathematical Modelling* 12, 471-81.
- Le Provost, C. and Vincent, P. (1986). "Some tests of precision for a finite element model of ocean tides," *Journal of Computational Physics* 65, 273-91.
- Luettich, R.A., Westerink, J.J., and Scheffner, N.W. (1992). "ADCIRC: An advanced three-dimensional circulation model for shelves, coasts and estuaries, Report 1: Theory and methodology of ADCIRC-2DDI and ADCIRC-3DL," Technical Report DRP-92-6, U.S. Army Engineer Waterways Experiment Station, Vicksburg, MS.
- Lynch, D.R., and Gray, W.G. (1979). "A wave equation model for finite element tidal computations," *Computers and Fluids* 7, 207-28.
- Lynch, D.R., and Werner, F.E. (1991). "Three-dimensional hydrodynamics in finite elements, Part II: Nonlinear timestepping," *Int. J. Numer. Methods Fluids* 12, 507-33.
- Lynch, D.R., Werner, F.E., Cantos-Figuerola, A., and Parilla, G. (1989). "Finite element modeling of reduced-gravity flow in the Alboran Sea: Sensitivity studies." *Seminario Sobre Oceanografia Fisica del Estrecho de Gibraltar*, Madrid, Spain, 283-95.
- Pearson F. (1990). *Map projections: Theory and applications*. CRC Press, Inc., Boca Raton, FL.
- Platzman, G.W. (1981). "Some response characteristics of finite element tidal models," *Journal of Computational Physics* 40, 36-63.
- Reid, R.O. (1990). "Waterlevel changes." *Handbook of Coastal and Ocean Engineering*. J. Herbich, ed., Gulf Publishing, Houston, TX.
- Schwiderski, E.W. (1979). "Global ocean tides, Part II: The semidiurnal principle lunar tide ( $M_2$ ), atlas of tidal charts and maps," NSWCR 79-414.

- Schwiderski, E.W. (1980). "On charting global ocean tides," *Reviews in Geophysics and Space Physics* 18, 243-68.
- \_\_\_\_\_. (1981a). "Global ocean tides, Part III: The semidiurnal principle solar tide ( $S_2$ ), atlas of tidal charts and maps," NSWC TR 81-122.
- \_\_\_\_\_. (1981b). "Global ocean tides, Part IV: The diurnal luni-solar declination tide ( $K_1$ ), atlas of tidal charts and maps," NSWC TR 81-142.
- \_\_\_\_\_. (1981c). "Global ocean tides, Part V: The diurnal principle lunar tide ( $O_1$ ), atlas of tidal charts and maps," NSWC TR 81-144.
- \_\_\_\_\_. (1981d). "Global ocean tides, Part VI: The semidiurnal elliptical lunar tide ( $N_2$ ), atlas of tidal charts and maps," NSWC TR 81-218.
- \_\_\_\_\_. (1981e). "Global ocean tides, Part VII: The diurnal principle solar tide ( $P_1$ ), atlas of tidal charts and maps," NSWC TR 81-220.
- \_\_\_\_\_. (1981f). "Global ocean tides, Part VIII: The semidiurnal luni-solar declination tide ( $K_2$ ), atlas of tidal charts and maps," NSWC TR 81-222.
- \_\_\_\_\_. (1981g). "Global ocean tides, Part IX: The diurnal elliptical lunar tide ( $Q_1$ ), atlas of tidal charts and maps," NSWC TR 81-224.
- Vincent, P. and Le Provost, C. (1988). "Semidiurnal tides in the Northeast Atlantic from a finite element numerical model," *Journal of Geophysical Research* 93(C1), 543-55.
- Wahr, J.M. (1981). "Body tides on an elliptical, rotating, elastic and oceanless earth," *Geophys. J.R. Astr. Soc.* 64, 677-703.
- Walters, R.A. (1988). "A finite element model for tides and currents with field applications," *Comm. Applied Numerical Methods* 4, 401-11.
- Walters, R.A. and Werner, F.E. (1989). "A comparison of two finite element models of tidal hydrodynamics using a North Sea data set," *Advances in Water Resources* 12(4), 184-93.
- Werner, F.E. and Lynch, D.R. (1989). "Harmonic structure of English Channel/Southern Bight tides from a wave equation simulation," *Advances in Water Resources* 12, 121-42.
- Westerink, J.J. and Gray, W.G. (1991). "Progress in surface water modeling," *Reviews of Geophysics* April Supplement, 210-17.

- Westerink, J.J., Luettich, R.A., Baptista, A.M., Scheffner N.W., and Farrar, P. (1992). "Tide and storm surge predictions using a finite element model," *Journal of Hydraulic Engineering* 118, 1373-90.
- Westerink, J.J., Luettich, R.A., and Scheffner, N.W. (1993). "ADCIRC: An advanced three-dimensional circulation model for shelves, coasts, and estuaries; Report 3, Development of a tidal constituent database for the Western North Atlantic and Gulf of Mexico," U.S. Army Engineer Waterways Experiment Station, Vicksburg, MS.
- Woodworth, P.L. (1990). "Summary of recommendations to the UK Earth Observation Data Centre (UK-EODC) by the Proudman Oceanographic Laboratory (POL) for tide model corrections on ERS-1 geophysical data records," Proudman Oceanographic Laboratory Communication.



# REPORT DOCUMENTATION PAGE

*Form Approved*  
OMB No. 0704-0188

Public reporting burden for this collection of information is estimated to average 1 hour per response, including the time for reviewing instructions, searching existing data sources, gathering and maintaining the data needed, and completing and reviewing the collection of information. Send comments regarding this burden estimate or any other aspect of this collection of information, including suggestions for reducing this burden, to Washington Headquarters Services, Directorate for Information Operations and Reports, 1215 Jefferson Davis Highway, Suite 1204, Arlington, VA 22202-4302, and to the Office of Management and Budget, Paperwork Reduction Project (0704-0188), Washington, DC 20503.

<b>1. AGENCY USE ONLY (Leave blank)</b>		<b>2. REPORT DATE</b> August 1994	<b>3. REPORT TYPE AND DATES COVERED</b> Report 4 of a series	
<b>4. TITLE AND SUBTITLE</b> ADCIRC: An Advanced Three-Dimensional Circulation Model for Shelves, Coasts, and Estuaries; Report 4, Hurricane Storm Surge Modeling Using Large Domains			<b>5. FUNDING NUMBERS</b> WU 32466	
<b>6. AUTHOR(S)</b> C.A. Blain, J.J. Westerink, R.A. Luetlich, Jr., N.W. Scheffner				
<b>7. PERFORMING ORGANIZATION NAME(S) AND ADDRESS(ES)</b> See reverse.			<b>8. PERFORMING ORGANIZATION REPORT NUMBER</b>  Technical Report DRP-92-6	
<b>9. SPONSORING / MONITORING AGENCY NAME(S) AND ADDRESS(ES)</b> U.S. Army Corps of Engineers Washington, DC 20314-1000			<b>10. SPONSORING / MONITORING AGENCY REPORT NUMBER</b>	
<b>11. SUPPLEMENTARY NOTES</b> Available from the National Technical Information Service, 5285 Port Royal Road, Springfield, VA 22161.				
<b>12a. DISTRIBUTION / AVAILABILITY STATEMENT</b> Approved for public release; distribution is unlimited.			<b>12b. DISTRIBUTION CODE</b>	
<b>13. ABSTRACT (Maximum 200 words)</b>  This report investigates the use of large domains in modeling hurricane storm surge. The hydrodynamic model used in this study is the ADCJIRC-2DDI code, which is based on a two-dimensional, depth-integrated, finite element formulation. Hurricane wind stress and pressure forcing from Hurricane Kate are produced by the HURWIN code, a vertically averaged planetary boundary layer wind model.  Storm surge predictions are conducted over three computational domains, which have varying sizes. The smallest domain covers the continental shelf, another domain includes the Gulf of Mexico, and the final domain is quite large and extends into the deep ocean. Domains over the continental shelf and the Gulf of Mexico are shown to be inadequate for modeling hurricane storm surge. On the contrary, a large domain, which includes the Western North Atlantic Ocean, the Caribbean Sea, and the Gulf of Mexico, is optimal for use with storm surge models. The influence of an inverted barometer condition applied at the open boundary is examined for each computational domain.  <div style="text-align: right;">(Continued).</div>				
<b>14. SUBJECT TERMS</b> See reverse.			<b>15. NUMBER OF PAGES</b> 63	
			<b>16. PRICE CODE</b>	
<b>17. SECURITY CLASSIFICATION OF REPORT</b> UNCLASSIFIED	<b>18. SECURITY CLASSIFICATION OF THIS PAGE</b> UNCLASSIFIED	<b>19. SECURITY CLASSIFICATION OF ABSTRACT</b>	<b>20. LIMITATION OF ABSTRACT</b>	

7. (Concluded).

U.S. Army Engineer Waterways Experiment Station,  
3909 Halls Ferry Road, Vicksburg, MS 39180-6199  
Department of Civil Engineering and Geological Sciences,  
University of Notre Dame, Notre Dame, IN 46556  
Institute of Marine Sciences, University of North Carolina  
at Chapel Hill, Morehead City, NC 28557

13. (Concluded).

Finally, storm surge simulations resulting from an application of wind, pressure, and tidal forcing over the large domain are compared to measured data. Five tidal constituents,  $K_1$ ,  $O_1$ ,  $P_1$ ,  $M_2$ , and  $S_2$  are forced both on the interior of the domain and along the open ocean boundaries. Initially, computed tidal elevations are compared with measured tidal data at 77 stations located throughout the domain with excellent results. For the storm surge predictions, an inverted barometer condition is also implemented along the open boundary. The resulting storm surge elevations predicted at eight stations along the Florida coast correlate well with measured storm surge elevations.

14. (Concluded).

Circulation model  
Finite element method  
Hurricane surge model  
Hydrodynamic model

Numerical model  
Storm surge model  
Two-dimensional model